Chapter 2. Spatial Patterns of Speciated $PM_{2.5}$ Aerosol Mass Concentrations

Characterizing the composition of major aerosol species is essential for estimating their contribution to $PM_{2.5}$ total mass concentration and visibility degradation. Analyzing the spatial variability of major aerosol species is important for understanding their sources and local and regional impacts. Data from the IMPROVE network are particularly useful for this type of analysis, given their spatial distribution and long temporal record. In addition to the mostly remote/rural sites operated by IMPROVE, the Chemical Speciation Network (CSN), operated by the Environmental Protection Agency (EPA), collects $PM_{2.5}$ speciated aerosol data at approximately 200 urban/suburban monitoring sites. Data from the IMPROVE and CSN networks are useful independently, but by combining data from the two networks, a more complete spatial analysis of key aerosol species can be explored as a function of geographical region by specifically exploring the differences in urban and rural aerosol signatures. In this section we examine the 2005–2008 annual mean mass concentrations of ammonium sulfate (AS), ammonium nitrate (AN), particulate organic matter (POM), light absorbing carbon (LAC), mineral soil aerosols, sea salt, and $PM_{2.5}$ gravimetric fine mass (FM) (we use $PM_{2.5}$ gravimetric mass and fine mass interchangeably in this report), as well as their contribution to $PM_{2.5}$ reconstructed fine mass (RCFM), PM_{10} (particles with aerodynamic diameters less than 10 μm from the EPA's PM_{10} network), and coarse mass (CM) (the difference between PM_{10} and $PM_{2.5}$ at IMPROVE sites only).

The CSN (a subset of which is formerly known as the Speciated Trends Network, or STN) was initiated in early 2000 with the purpose of identifying sources, developing implementation plans, and supporting ongoing health-effects research. Currently, it operates approximately 200 sites in mostly urban and suburban locations. The CSN has operated many different samplers, depending on the site, including the Andersen Reference Ambient Air Sampler (RAAS), MetOne SASS, URG, R&P2300, and R&P2025. The flow rates and face velocities of these samplers can differ significantly from the IMPROVE sampler, which could lead to differences in concentrations, especially for carbon. CSN now mostly operates the MetOne and the URG3000N. For most species, CSN and IMPROVE measurements and analyses are similar (see section 1.4 for a comparison of data from collocated sites). Both networks maintain a one-in-three-day sampling frequency (some CSN sites are one-in-six day). CSN cold-ships their samples while IMPROVE does not . As discussed in section 1.4, samples for gravimetric and elemental analyses are collected with Teflon filters. Gravimetric mass is determined using electro-microbalance techniques, and energy dispersive X-ray fluorescence is used for trace elements. Samples for ion chromatography analysis are collected using nylon substrates, and samples for carbon analyses are collected on quartz fiber substrates. The major difference between the analyses performed by IMPROVE and the CSN had been the determination of organic carbon (OC) and LAC[1]. IMPROVE uses thermal optical reflectance (TOR) and the CSN uses thermal optical transmission (TOT), both of which are known to produce similar total carbon concentrations but different splits between OC and LAC (Chow et

[1] The CSN network changed the sampler and analysis method for carbonaceous $PM_{2.5}$ monitoring beginning in the spring of 2007 to be more compatible with the methods used by IMPROVE. For more information see http://www.epa.gov/ttn/amtic/specurg3000.html

al., 2004). In addition, the CSN applies the NIOSH-like (National Institute for Occupational Safety and Health) analysis protocol that differs from the IMPROVE protocol for determining the split between OC and LAC. Furthermore, the handling of carbon sampling artifacts is different between the networks. Positive artifacts are associated with adsorption of organic gases onto the filter, and negative artifacts occur due to volatilization of particulate organics (Turpin et al., 2000). While blank corrections for the positive artifact are routinely applied to IMPROVE carbon data, they are not applied routinely as part of the CSN protocol; however they can be found elsewhere (www.epa.gov/airexplorer). More discussion of the carbon data comparisons can be found in section 2.1.3, including a discussion of new artifact corrections for CSN data used for this report.

Data from a 4-year time period (2005–2008) are examined in this chapter. To ensure that the data are representative of the entire time period, certain completeness criteria first were applied. Fifty percent completeness of the data (two years of valid monthly mean data) for a given site was required to be included in the analysis. Half of the total observations in a given month had to be valid for a monthly mean. In addition, 66% of each 3-month season was required for an annual mean (a total of 8 months, but represented across each season, were required for an annual mean). Seasons correspond to winter (December, January, February), spring (March, April, May), summer (June, July, August) and fall (September, October, November). These criteria were applied for each species separately. Values below the minimum detection limit (MDL) were handled according to how they were reported by each network, i.e., we made no additional corrections for values below MDLs. For IMPROVE, ion and carbon data were reported below their MDLs. XRF data were reported as zero if they were below MDLs. Data from the CSN were handled similarly. Average reconstructed mass calculations were performed by summing the averages; for example, an average concentration of each species was computed and summed to obtain an average RCFM. Valid data for all of the species were required to compute monthly mean RCFM, with the exception of sea salt. This approach was used to avoid small sample sizes and provide a more accurate representation of average conditions. Applying the completeness criteria resulted in 168 IMPROVE sites and 176 CSN sites used in the analyses.

Maps of monthly mean and annual mean concentrations were created for each species from sites that met the completeness criteria. A Kriging algorithm was used to interpolate concentrations between site locations in order to create concentration isopleths.Maps based on interpolation schemes should be viewed and interpreted with caution. The maps are intended to help visualize the data and identify large spatial patterns only. The density of site locations obviously affects the interpolated fields, and neither the IMPROVE nor CSN networks have uniformly distributed site locations around the United States. Given this caveat, there is still interesting and useful information that can be gained from these maps, especially by examining the differences that occur when maps based only on the rural/remote IMPROVE network are compared to those created when integrating the urban/suburban CSN data with IMPROVE data. The following sections include discussions of spatial patterns for annual mean concentrations of AS, AN, POM, LAC, soil, sea salt, FM, the difference between FM and RCFM, coarse mass (IMPROVE only), and PM_{10} mass. The top number in the scale shown on each contour map corresponds to the maximum concentrations for all sites, although the contour levels themselves were created with the highest level corresponding to the 95^{th} percentile in mass concentration. Maps of species percent contribution to RCFM are also included. Tables listing 2005–2008

annual mean concentrations as a function of site for the IMPROVE network and the CSN are provided in Appendix B.1. Annual mean $PM_{2.5}$ mass fractions are listed according to site for the IMPROVE network and the CSN in Appendix B.2.

2.1 AEROSOL SPECIES COMPOSITION

In order to reconstruct $PM_{2.5}$ mass concentrations, assumptions about the molecular form of assumed species must be made. Table 2.1 presents the assumptions used in this report and those applied in previous report. More detail regarding each species will be presented in the following sections. Similar assumptions were made for IMPROVE and CSN unless otherwise noted in Table 2.1.

Table 2.1. Form of molecular species assumed in this report.

$PM_{2.5}$ Aerosol Species	**Previous Report**	**This Report**	**Assumptions**
Ammonium Sulfate (AS = $(NH_4)_2SO_4$)	4.125[S]	1.375[SO_4^{-2}]	Sulfate [SO_4^{-2}] is assumed to be fully neutralized. Previous assumptions used sulfur (S).
Ammonium Nitrate (AN = NH_4NO_3)	Same	1.29[NO_3^-]	Nitrate [NO_3^-] is assumed to be ammonium nitrate.
Particulate Organic Matter (POM)	1.8[OC]	1.8[OC]	Derived from organic carbon (OC) assuming average organic molecule is 55% carbon. Previous assumptions used a 1.4 factor.
Light Absorbing Carbon (LAC)	Same	LAC	Also referred to as EC in previous reports.
CSN POM	NA	1.8[OC]	Mathematically adjusted to compare with IMPROVE POM.
CSN LAC	NA	LAC	Mathematically adjusted to compare with IMPROVE LAC.
Sea Salt	Not considered.	1.8[Cl^-]	Sea salt is 55% chloride ion by weight. Previously not considered.
CSN Sea Salt	NA	1.8[Cl]	Sea salt is derived using chlorine concentrations from XRF.
Soil	Same	2.2[Al] + 2.49[Si] + 1.63[Ca] + 2.42[Fe] + 1.94[Ti]	Soil potassium = 0.6[Fe]. Fe and Fe_2O_3 are equally abundant. A factor of 1.16 is used to account for other compounds such as MgO, Na_2O, H_2O and CO_3.
Gravimetric $PM_{2.5}$ Mass (FM)	Same	$PM_{2.5}$	A $PM_{2.5}$ cut point on the fine mass sample.
Coarse Mass (CM)	Same	PM_{10} - $PM_{2.5}$	PM_{10} cut point on the mass sample.
IMPROVE PM_{10}	Same	PM_{10}	PM_{10} cut point.
EPA PM_{10}	NA	PM_{10}	PM_{10} cut point.
Reconstructed Fine Mass (RCFM)	[AS]+[AN]+[POM]+[LAC]+[Soil]	AS + AN + POM + LAC + Soil + Sea Salt	Represents $PM_{2.5}$ fine aerosol mass, including sea salt.
Mass Difference (dM)	NA	FM - RCFM	

2.1.1 $PM_{2.5}$ Ammonium Sulfate Mass Concentrations

The majority of sulfate in the atmosphere is produced through chemical reactions of sulfur dioxide (SO_2). Anthropogenic SO_2 is emitted through industrial activities such as coal and diesel fuel combustion. Regions that host electric utilities and industrial boilers (such as the eastern United States) are sources of SO_2 emissions that, combined with the elevated relative humidity or other aqueous pathways, create the most efficient conditions for sulfate production. The degree of acidity of sulfate (from acidic sulfuric acid to fully neutralized AS) depends on the availability of ammonia to neutralize the sulfuric acid formed from SO_2. Sulfate acidity can vary spatially and temporally (e.g., Gebhart et al., 1994; Liu et al., 1996; Day et al., 1997; Lowenthal et al., 2000; Lefer and Talbot, 2001; Quinn et al., 2002a; Chu et al., 2004; Hogrefe et al., 2004; Schwab et al., 2004; Tanner et al., 2004; Zhang et al., 2005), but without additional measurements of ammonium ion concentration, the degree of neutralization is unknown. We therefore assumed sulfate is in the form of fully neutralized AS (see Table 2.1), an upper bound of mass associated with dry sulfate.

2.1.2 $PM_{2.5}$ Ammonium Nitrate Mass Concentrations

Ammonium nitrate (AN) forms from the reversible reaction of gas-phase ammonia and nitric acid. Sources of oxidized nitrogen include combustion of fossil fuels from point sources such as coal-fired powered plants, on-road mobile sources and non-road mobile sources. Other high-temperature processes such as biomass burning also contribute oxidized nitrogen, as do biogenic sources such as soil emissions (Vitousek et al, 1997). Sources of ammonia include agricultural activities including animal husbandry, as well as mobile sources and natural emissions. The equilibrium reactions producing particle phase AN are sensitive to small changes in temperature and relative humidity that can shift the equilibrium between the particle and gas phase. Lower temperatures and higher relative humidity favor particulate AN, while higher temperatures and lower relative humidity favor the gas phase. Nitrate (as AN) is often assumed to be in the fine mode, and this is probably a reasonable assumption in regions with high ammonia and nitric acid concentrations and low sulfate concentrations. However, Lee et al. (2008) showed that in many locations nitrate is associated with the coarse mode from reactions of gas-phase nitric acid with sea salt or calcium carbonate. In these situations the nitrate measured in the fine mode is actually the tail of coarse-mode nitrate. Using data reported by Lee et al. (2008), Hand and Malm (2006) found that when fine mode nitrate concentrations were greater than 0.5 $\mu g\ m^{-3}$, AN contributed over 70% of the observed total nitrate in the fine mode at certain locations. For the purposes of reconstructing fine mass and light extinction coefficients, and because the necessary measurements to determine the form of nitrate are not regularly available, we assumed nitrate is in the form of AN.

2.1.3 $PM_{2.5}$ Particulate Organic Matter and Light Absorbing Carbon Mass Concentrations

The sources of POM in the atmosphere are both primary emissions and secondary formation. Primary emissions include particle mass emitted directly from combustion of fossil fuels or biomass. Secondary organic aerosols form in the atmosphere from the oxidation of gas-phase precursors from both anthropogenic and biogenic sources. Accurate estimates of POM are required in order to compute $PM_{2.5}$ mass closure and to estimate optical properties such as light scattering coefficients. Estimating the contributions of organic carbon (OC) aerosol to mass or

scattering requires an estimate of the total mass associated with OC. The OC multiplier (R_{oc}) used to estimate particulate organic material is an estimate of the average molecular weight per carbon weight for OC aerosol and takes into account contributions from other elements associated with the organic matter, such as N, O, and H. It is spatially and temporally variable. Typical values range from 1.2 to 2.6 (Turpin and Lim, 2001; El-Zanan et al., 2005). It is impossible to determine which and how many elements are associated with POM without knowing the chemical formula of the organic compound, and it is common for ~20–40% of organic aerosol mass to remain unidentified (Turpin and Lim, 2001). Because the organic compounds that compose POM are largely unknown, the approach for taking into account other elements in POM mass has been to apply an average multiplier. As Turpin and Lim (2001) review, the often-used value of 1.4 dates back to samples collected in Pasadena in the early 1970s and 1980s (Grosjean and Friedlander, 1975; White and Roberts, 1977; Van Vaeck and Van Cauwenberghe, 1978; Countess et al., 1980; Japar et al., 1984). Turpin and Lim (2001) have reviewed several estimates of R_{oc} in terms of the types of compounds known to compose POM, and to summarize their findings, they recommend a factor of 1.6 ± 0.2 for urban organic aerosols, a factor of 2.1 ± 0.2 for nonurban organic aerosols, and values ranging from 2.2 to 2.6 for samples with impacts from biomass burning. As part of the IMPROVE equation assessment that occurred in 2006, the value of 1.4 was deemed too low based on a summary of current literature. Instead, a value of 1.8 was recommended based on available data (Malm and Hand, 2007) and is applied here. Further examination of the multiplier is presented in Chapter 8 (Malm et al., 2011).

LAC, also referred to as black carbon, elemental carbon, graphitic carbon or soot, is produced directly through emission from incomplete combustion of fossil fuels or biomass (fires). LAC is the most abundant light-absorbing particle in the atmosphere in the visible spectrum. A comprehensive review of light absorption by LAC was provided by Bond and Bergstrom (2006). We use the term “light absorbing carbon” instead of elemental carbon (EC) to reflect the transition to this term in the scientific literature because of the operational definition, and sometimes morphology, associated with EC (Bond and Bergstrom, 2006; Malm et al., 1994). Light absorbing carbon particles may evolve in high temperature environments but not be graphitic (e.g., Hand et al., 2005). Replacing EC with LAC avoids potential confusion regarding the type of carbon particles responsible for light absorption.

Prior to 2007 the IMPROVE and CSN networks employed different samplers, analytical methods, and data processing routines for measuring total particulate carbon and the organic and LAC fractions. One of the major differences between the networks is the treatment for sampling artifacts. Positive artifacts occur when organic gases are trapped by the quartz filters used for sampling and can induce a bias of ~50% of OC mass. Negative artifacts occur when particulate species are volatilized from the filter, resulting in losses of -80% (Turpin, 2000). One significant difference between the CSN and IMPROVE is that IMPROVE reports carbon concentrations that have been corrected for positive artifacts while the CSN does not make adjustments to the data reported to the EPA air quality system (AQS, http://www.epa.gov/ttn/airs/aqsdatamart/). Differences in the face velocities of the various samplers operated by IMPROVE and the CSN lead to discrepancies in concentrations due to negative and positive artifacts. In addition, the CSN applies the NIOSH-like protocol and TOT analysis (Chow et al., 2004), while IMPROVE applies its own sampling protocol and TOR to determine carbon fractions. Differences of up to 30% in LAC concentrations have been reported due to the TOR versus TOT method (TOR

larger, Chow et al., 2004). These differences in sampling and analysis lead to discrepancies between carbon concentrations reported by the two networks.

To combine the carbon data between the IMPROVE and CSN networks, we applied corrections to the CSN carbon data, based on comparisons of data from collocated CSN and IMPROVE samplers, to account for all of the differences described above. We used data from twelve urban monitoring sites with collocated samplers for the time period of 2005–2006. CSN total carbon concentrations (TC) were systematically higher than IMPROVE TC, with the magnitude of the biases dependent on the CSN sampler type but independent of monitoring site. A linear regression of TC from the two networks resulted in a positive intercept in the CSN data that indicated an additive bias that was most likely associated with a positive OC artifact. The sampler dependence appeared to be related to the sampler operating conditions (e.g., flow rate and face velocity) because the closest agreement occurred for the CSN sampler that was most similar to the IMPROVE sampler. A sampler-dependent multiplicative bias was also evident, with the bias increasing with increasing face velocity. The multiplicative bias was interpreted as a negative organic artifact associated with the loss of semivolatile OC species due to the pressure drop across the filter. In contrast to TC, IMPROVE LAC concentrations were systematically higher than CSN LAC, consistent with the known differences in TOR versus TOT methods (Chow et al., 2004). The biases were multiplicative, suggesting analytical biases. No additive bias was observed, consistent with minimal LAC measured on back up filters (Eldred, 2002). These comparisons were used to derive monthly correction factors that were applied to the CSN data. A detailed description of the derivation of data corrections and the resulting concentration comparisons can be found in Chapter 8 and Malm et al. (2011). Equations 2.1 and 2.2 were used to adjust the CSN OC and LAC data:

$$LAC_{adj}=1.3(LAC_{CSN}) \quad 2.1$$

$$OC_{adj}=\frac{OC_{CSN}-0.3LAC_{CSN}-A}{M} \quad 2.2$$

LAC_{adj} and OC_{adj} refer to the adjusted CSN LAC and OC data, respectively, and were used in the analyses presented in this report. The adjustements were applied as a function of month and sampler. The top row of Table 2.1.3 lists the multiplicative negative artifact (M) as a function of CSN sampler. The columns of Table 2.1.3 list the additive positive organic artifact (A) as a function of month and sampler.

Table 2.1.3. The negative multiplicative artifact (M) and the monthly positive additive organic artifact (A_{month}) used to adjust the CSN carbon concentrations for comparisons with IMPROVE. The units for the positive artifacts are μg m^{-3} and M is unitless. Adjustments are listed as a function of sampler (columns).

	MetOne	Anderson	URG	R&P-2300	R&P-2025
M	1.2	1.2	1.1	1.1	1.1
A_{Jan}	1.1	0.92	0.24	1.2	0.24
A_{Feb}	1.3	1.1	0.27	1.4	0.27
A_{Mar}	1.2	1.0	0.26	1.4	0.26
A_{Apr}	1.4	1.2	0.29	1.5	0.29
A_{May}	1.6	1.3	0.33	1.7	0.33
A_{Jun}	1.7	1.4	0.35	1.8	0.35
A_{Jul}	1.8	1.5	0.38	2.0	0.38
A_{Aug}	1.9	1.6	0.41	2.1	0.41

	MetOne	Anderson	URG	R&P-2300	R&P-2025
A_{Sep}	1.5	1.2	0.31	1.6	0.31
A_{Oct}	1.2	0.90	0.23	1.2	0.23
A_{Nov}	1.0	0.85	0.22	1.1	0.22
A_{Dec}	1.1	0.89	0.23	1.2	0.23

Scatter plots of original and corrected data are presented in the detailed discussion in Chapter 8 and Malm et al. (2011) and in Appendix A. In the spring of 2007 the CSN began converting its carbon samplers to URG model 3000N samplers and applying TOR analysis using the IMPROVE protocol for carbon measurements in an effort to converge toward an IMPROVE-like measurement. These data were used for the sites where they were available. The only adjustments made to the IMPROVE-like CSN data were a positive artifact correction to OC concentrations. Although this artifact is most likely seasonal, a constant correction of 0.3 μg m^{-3} was applied based on carbon artifact investigations for IMPROVE quartz filters (Eldred, 2002).

2.1.4 $PM_{2.5}$ Soil Mass Concentration

Sources of soil dust in the atmosphere include entrainment from deserts, paved and unpaved roads, agricultural activity, construction, and fire (Seinfeld and Pandis, 1998). Deposition of dust usually corresponds to large particles that settle near their source regions, although there are many exceptions. Several studies have shown that contributions of Asian dust to U.S. fine soil concentrations can be significant episodically, affecting aerosol concentrations and mineralogy across the United States, typically in the spring (e.g., Husar et al., 2001; Prospero et al., 2002; VanCuren and Cahill, 2002; Jaffe et al., 2003; VanCuren, 2003). Transport of North African dust to the United States occurs regularly in summer, affecting aerosol concentrations in the Virgin Islands, the eastern and southeastern United States (Perry et al., 1997), and even as far west as Big Bend, Texas (Hand et al., 2002). Soil concentrations in desert regions of the Southwest are expected to be higher due to the impacts of local sources as well as transboundary transport from the Chihuahuan desert in Mexico, especially in winter and spring (Rivera Rivera et al., 2009).

Fine soil as characterized by $PM_{2.5}$ samplers most likely corresponds to the fine tail of the coarse mode. Variability in soil concentrations could be due to changes in the magnitudes of mass concentrations for a given size mode or to shifting size distribution that results in more or less mass available in the fine mode size range. Due to the spatial and temporal variability in dust sources, it is very difficult to characterize an appropriate aerosol soil composition for each measurement site. Soil mass concentrations are therefore estimated by a general method that sums the oxides of elements that are typically associated with soil (Al_2O_3, SiO_2, CaO, K_2O, FeO, Fe_2O_3, TiO_2), with a correction for other compounds such as MgO, Na_2O, H_2O and carbonates (Malm et al., 1994). Elemental concentrations are multiplied by factors that represent the mass concentrations of the oxide forms. Several corrections are also made. Molar concentrations of iron are assumed to be equally abundant in the forms of FeO and Fe_2O_3. Potassium has a nonsoil contribution from biomass smoke, so the soil potassium is estimated by using Fe as a surrogate, or *[K] = 0.6[Fe]*. The formula for computing soil concentration is given in Table 2.1 and has been divided by 0.86 to take into account missing compounds.

Comparisons of IMPROVE and CSN data performed for this report (see section 1.4) and those performed previously (Debell et al., 2006) suggested that relative biases of up to 30% or

more in soil concentrations between collocated IMPROVE and CSN samplers existed, with higher IMPROVE concentrations. In addition, analyses of IMPROVE data suggested that $PM_{2.5}$ soil mass concentrations may be underestimated by as much as 20% and have some regional dependence (Malm and Hand, 2007). Given these uncertainties, the combination of IMPROVE and CSN soil concentrations should be interpreted as semiquantitative.

2.1.5 $PM_{2.5}$ Sea Salt Mass Concentration

Sea salt can be a significant fraction of the RCFM at many coastal locations, (e.g., the Virgin Islands), as well as contribute significantly to light scattering (e.g., Quinn et al., 2001, 2002b, 2004). Sea salt concentrations are typically computed from sea salt markers like the sodium ion, chloride ion, or combination of ions (Quinn et al., 2001). Difficulties in computing sea salt from data from the IMPROVE network arise because positive ions are not analyzed; therefore sodium ion data (the strongest indicator of sea salt) are not available. Elemental sodium data are available from XRF analyses; however, sensitivity issues regarding poor detection of Na result in large uncertainties corresponding to Na from XRF (White, 2008). Issues also arise when using the chloride ion or chlorine to estimate sea salt because the reaction of gaseous nitric acid with sea salt produces sodium nitrate particles and the release of gaseous HCl. The depletion of chloride during this reaction results in an underestimation of sea salt when using chloride to compute it. However, given these limitations, it was proposed that calculations for reconstructing mass include sea salt by multiplying the chloride ion (Cl^-) by 1.8 (sea salt is 55% Cl by weight as defined by the composition of sea water by Seinfeld and Pandis, 1998). Because the chloride ion is not analyzed by the CSN, sea salt is computed using the 1.8 factor multiplied by chlorine as measured by XRF. Comparisons of sea salt concentrations between collocated CSN and IMPROVE sites (see section 1.4) suggested that IMPROVE concentrations were up to three times higher on average compared to CSN, with a relative bias of 63%. Given these disparities in concentrations, the integration of CSN and IMPROVE sea salt data should be interpreted with caution.

2.1.6 $PM_{2.5}$ Gravimetric Fine Mass and Reconstructed Fine Mass

Gravimetric fine mass concentrations (FM) are determined gravimetrically by pre- and post-weighting of Teflon filters. The filters are equilibrated to 20–23 degrees C and 30–40% relative humidity. Teflon filters have known sampling artifacts. For example, nitrate loss and volatilization of some organic species contribute to negative artifacts (Hering and Cass, 1999; Ashbaugh and Eldred, 2004; Frank, 2006), while positive artifacts correspond to retention of water associated with acidic species (Frank, 2006).

Reconstructed fine mass is the sum of AS, AN, POM, LAC, soil, and sea salt. RCFM should equal FM if the assumptions regarding molecular forms of species are appropriate and if there are minimal biases associated with the measurements.

2.1.7 $PM_{2.5}$ Mass Difference

Differences in FM and RCFM (dM = FM - RCFM) were computed to investigate the degree to which the algorithm for computing RCFM was capturing the FM concentrations. Some of the differences were related to the sampling artifacts associated with FM discussed earlier,

such as loss of volatile species or retained water on the filter. In addition, incorrect molecular forms of assumed species could have contributed. More acidic forms of sulfate, nitrate species other than AN, different OC multipliers, or soil formulas could have contributed to differences between FM and RCFM. A detailed investigation into biases associated with FM measurements is presented in Chapter 8 and Malm et al. (2011).

2.1.8 PM_{10} and Coarse Mass Concentrations

Coarse mass (CM) is the difference between gravimetric PM_{10} and $PM_{2.5}$ mass concentrations (PM_{10} - $PM_{2.5}$) measured gravimetrically and is not routinely analyzed for speciation. To investigate the speciation of CM, a coarse particle speciation network was initiated at nine IMPROVE sites in 2003. Sites were selected to be representative of the continental United States and were operated according to IMPROVE protocol analytic procedures for a period of one year, with additional A, B, and C modules operating with PM_{10} inlets. Malm et al. (2007) reported that soil (as defined by the IMPROVE soil equation) was the largest contributor to CM at most sites and ranged from 34% at Mount Rainier National Park to 76% at Grand Canyon National Park. With the exception of Mount Rainier, annual average soil contributions to CM were higher in the western United States. POM was the next highest contributor, ranging from 9% at Grand Canyon National Park to 59% at Mount Rainier National Park. Nitrate was next highest contributor (4–12%), probably associated with sea salt on the coast and dust in the inner and western areas of the country (Lee et al., 2008). Sulfate was a minor contributor to CM, with its fractional contribution less than a few percent. The optical, physical, chemical, and hygroscopic properties of coarse-mode aerosols can vary significantly, depending on the composition and size distribution of CM, and could have important implications to total scattering, because in some remote areas contributions to total scattering from the coarse-mode scattering could be comparable to fine-mode contributions. For example, there were several periods in Big Bend, Texas when up to 80% of total scattering was attributable to the coarse mode (Hand, 2001; Hand et al., 2002).

PM_{10} concentrations are not measured routinely as part of the CSN protocol, so no CM estimation could be made for urban sites. However, the EPA maintains a large network of PM_{10} samplers at over 700 sites around the United States. Several of these sites are collocated with CSN sites. Instead of introducing errors by interpolating PM_{10} concentrations to CSN sites with no collocated PM_{10} sampler, we compared PM_{10} concentrations, instead of CM concentrations, for IMPROVE and EPA monitors to investigate the rural and urban differences in PM_{10}.

2.2 SPATIAL PATTERNS IN ANNUAL MEAN MASS CONCENTRATIONS

2.2.1 $PM_{2.5}$ Ammonium Sulfate Mass

The rural 2005–2008 IMPROVE annual mean AS concentrations ranged from 0.36 μg m^{-3} in Petersburg, Alaska (PETE1), to 6.11 μg m^{-3} in Livonia, Indiana (LIVO1). The combination of high SO_2 emissions and high relative humidity produced the highest concentrations (4–6 μg m^{-3}) of AS in the eastern United States that centered on the Ohio River valley and Appalachia regions (see Figure 2.2.1a). The concentrations of AS decreased sharply in the surrounding regions of the country. In fact, concentrations in the western United States were typically less than 2 μg m^{-3}, with the lowest concentrations in the Northwest and in

Montana and Idaho. The low concentrations of AS that corresponded to most of the IMPROVE sites was a consequence of site location; around 62% of IMPROVE sites are located in the western half of the country (west of -100º), where SO_2 emissions are lower.

The regional impact of AS concentrations was evidenced by the similar concentrations of AS at the urban CSN sites. A maximum CSN concentration of 8.01 μg m^{-3} occurred in southwestern Pennsylvania (Liberty, #420030064), similar to the maximum concentration observed in the IMPROVE network. Most of the CSN sites had AS concentrations greater than 2 μg m^{-3}, due to the fact that the majority of CSN sites are located in the East (80% of CSN sites are east of -100º). The lowest concentration (0.75 μg m^{-3}) occurred at La Grande (#410610119) in eastern Oregon. The spatial distribution of AS with the rural and urban sites combined (see Figure 2.2.1b) was very similar to the pattern of the rural sites alone, suggesting that regional impacts of high AS concentrations in the East influenced both urban and rural sites similarly. The addition of urban sites in the Ohio River valley provided some additional structure in the isopleths in Figure 2.2.1b but did not alter the overall pattern considerably.

RCFM was primarily composed of AS in the eastern United States (see Figure 2.2.1c). IMPROVE AS mass fractions above 50% occurred for 19 sites in the eastern and northeastern United States, and the spatial pattern of AS mass fraction was similar to that of AS mass concentrations with some exceptions. For example, the Northeast had high mass fractions even though the AS concentrations were fairly low (especially compared to the mid-South and Southeast), suggesting that these regions had fairly low concentrations of AS but that the RCFM is still dominated by AS. These differences were also observed in the West. Higher mass fractions extend into west Texas due to the Big Bend NP site (BIBE1), where the influence of AS to RCFM has been well documented (Lee et al., 2004; Barna et al., 2006; Gebhart et al., 2006; Schichtel et al., 2006). The fraction of AS in the central United States approached 40% and declined to the west, with the lowest fractions (10–15%) in the Northwest. The highest IMPROVE AS fraction actually occurred in Hawaii Volcanoes NP (HAVO1, 79.2%), most likely due to the high levels of emissions of SO_2 during eruptions in March of 2008 that signaled a new phase of activity at the Halema`uma`u Crater (http://www.nps.gov/havo/planyourvisit/halemaumau_newgasvent.htm). The lowest fraction occurred in northern California site of Trinity (9.7%, TRIN1).

The spatial pattern of AS mass fraction for rural plus urban sites was similar to the rural sites alone (Figure 2.2.1d), especially in the East. The highest urban mass fraction was less than the maximum rural mass fraction and occurred in Charleston, West Virginia (60.0%, #540390011); the lowest mass fraction (5.6%) occurred in northwestern Montana (Libby, #300530018). The AS mass fraction in many urban centers was lower than the surrounding urban area (e.g., Salt Lake City, Denver, and the Eastern Seaboard). As will be shown in the next sections, these gradients were mostly likely due to the higher contributions of ammonium nitrate (AN) and carbonaceous aerosols in urban versus rural sites. The inclusion of urban sites in the interpolation scheme often adjusted the spatial patterns to account for the additional information. For example, in Texas and the Gulf states, regions along the coast had higher mass fractions compared to the rural map due to the addition of sites in this region. This change in spatial patterns emphasizes the caution that must be applied when examining these types of maps. The similarity in the urban and rural AS concentrations and fractions of RCFM demonstrates the

regional impact of the sources and atmospheric processes that lead to elevated levels of AS in the atmosphere.

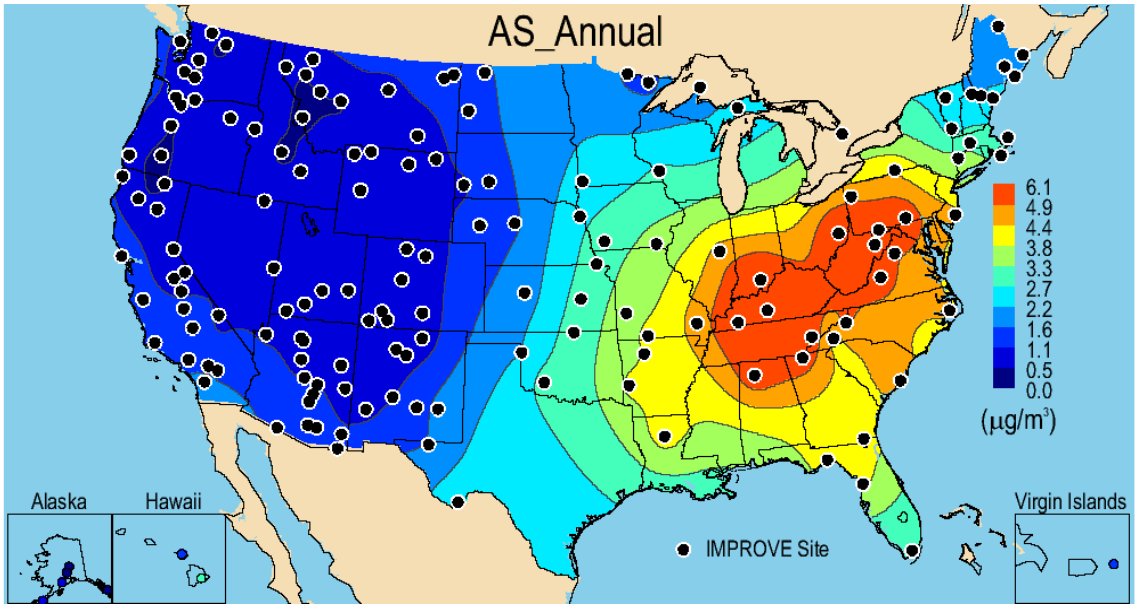

Figure 2.2.1a. IMPROVE (rural) 2005–2008 $PM_{2.5}$ ammonium sulfate (AS) annual mean mass concentrations (µg m^{-3}).

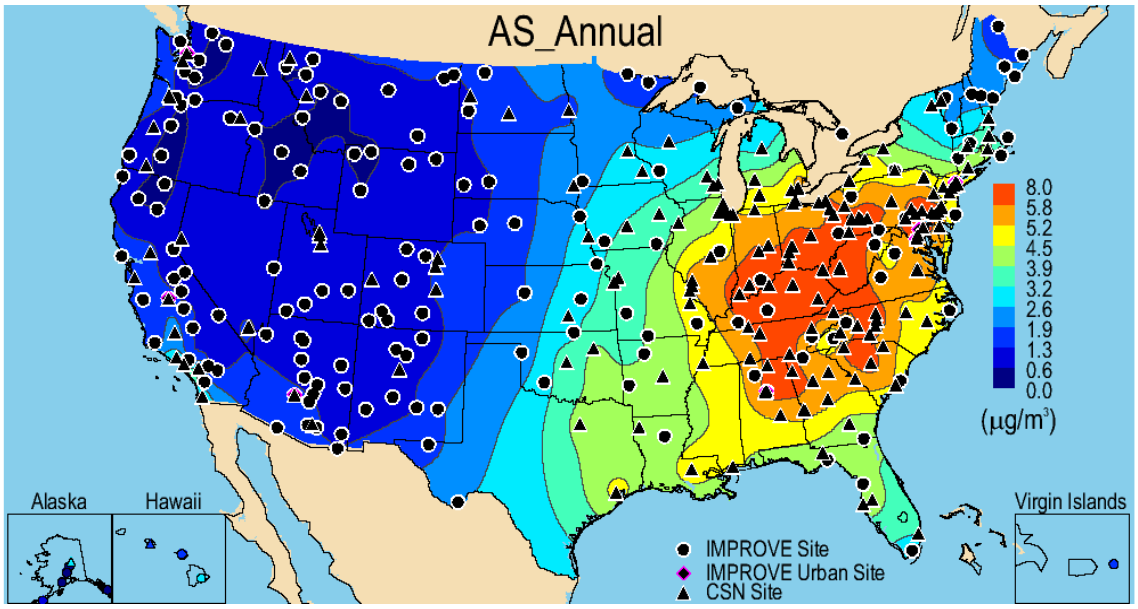

Figure 2.2.1b. IMPROVE and CSN 2005–2008 $PM_{2.5}$ ammonium sulfate (AS) annual mean mass concentrations (µg m^{-3}).

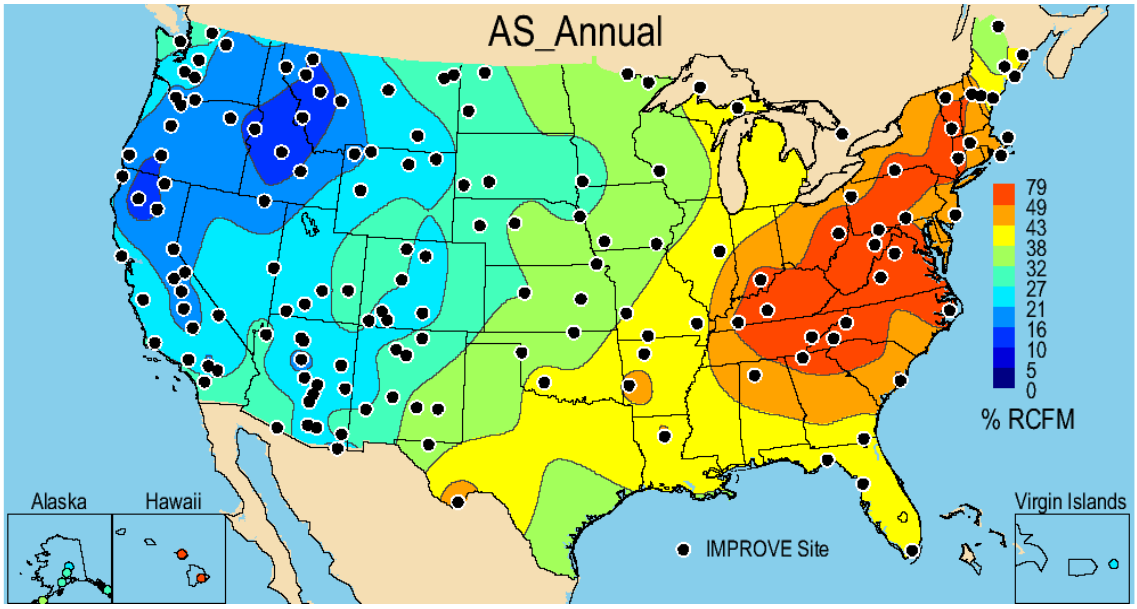

Figure 2.2.1c. IMPROVE (rural) 2005–2008 annual mean percent (%) contributions of ammonium sulfate (AS) to $PM_{2.5}$ reconstructed fine mass (RCFM).

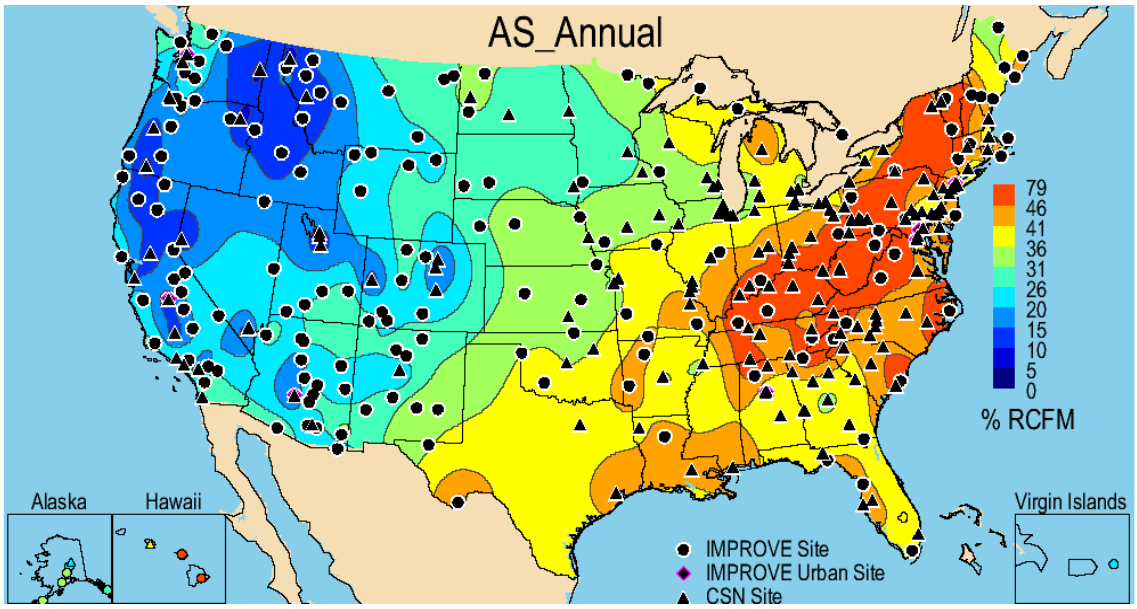

Figure 2.2.1d. IMPROVE and CSN 2005–2008 annual mean percent (%) contributions of ammonium sulfate (AS) to $PM_{2.5}$ reconstructed fine mass (RCFM).

2.2.2 $PM_{2.5}$ Ammonium Nitrate Mass

The AN "bulge" in the central/midwestern United States has been reported previously by Pitchford et al. (2009). Not surprisingly, locations where ammonia and nitric acid emissions were the highest correspond to the regions where AN concentrations were the largest (see Figure 2.2.2a). The maximum IMPROVE 2005–2008 rural concentration of 2.79 μg m^{-3} occurred at Bondville, Illinois (BOND1), a site located in the agricultural Midwest. The lowest rural concentration occurred in Petersburg, Alaska (0.04 μg m^{-3}, PETE1). Seven sites in the central United States had annual AN concentrations greater than 2 μg m^{-3}. Urban IMPROVE sites also

corresponded to higher AN concentrations. The annual AN concentration at the Fresno site (FRES1) was almost 2.5 times higher than even those in the central United States (6.47 μg m^{-3}). Surrounding rural sites, such as Sequoia NP (SEQU1) seemed to be influenced by urban AN, with an annual mean AN concentration of 2.11 μg m^{-3}. All of the other IMPROVE urban sites corresponded to concentrations between 1 and 2 μg m^{-3}, including Phoenix (PHOE1), New York City (NEYO1), Birmingham (BIRM1), Puget Sound (PUSO1), and Washington, D.C. (WASH1). Concentrations were much lower outside of the central United States and urban IMPROVE areas; the majority of the sites around the country had concentrations less than 0.5 μg m^{-3}.

The inclusion of CSN sites provided more structure to the AN spatial pattern and showed the impact of urban AN concentrations on surrounding areas (Figure 2.2.2b). The central "bulge" extended to include sites surrounding Lake Michigan. AN concentrations at sites in Michigan, Illinois, Wisconsin, and Indiana were typically 3–4 μg m^{-3}. Urban sites in the Northeast also had higher AN concentrations compared to the rural sites. In California, particularly Rubidoux (#060658001), annual concentrations reached 9.16 μg m^{-3}, and several other California sites had concentrations above 6 μg m^{-3}. The lowest CSN AN concentration occurred at Pearl City, Hawaii (0.26 μg m^{-3}, #150032004). Generally, urban concentrations of AN were considerably higher than rural concentrations.

Sites with high concentrations of AN were also in regions where a considerable fraction of the RCFM was composed of AN. The central U.S. and California sites were an example, with an AN RCFM fraction of 25% (Figure 2.2.2c). The rural IMPROVE site at Blue Mounds, Minnesota (BLMO1) had the highest annual contribution of AN to RCFM (31.6%), compared to the lowest at Sawtooth, Idaho (2.0 %, SAWT1). In general, however, most rural IMPROVE sites were not highly influenced by AN contributions to RCFM. The maximum fraction of AN at an urban IMPROVE site occurred at Fresno (35.6%, FRES1), compared to the lowest at Birmingham (5.8%, BIRM1) (Figure 2.2.2d). With the addition of the urban CSN sites, the influence of the contribution of AN to RCFM extended farther west from the central United States, where sites in Colorado and Utah ranged from 25 to 30% AN, and sites in California ranged up to 42.7% (Rubidoux, California, #060658001). The lowest urban CSN fraction occurred in the southern Georgia city of Douglas (#130690002, 4.3%).

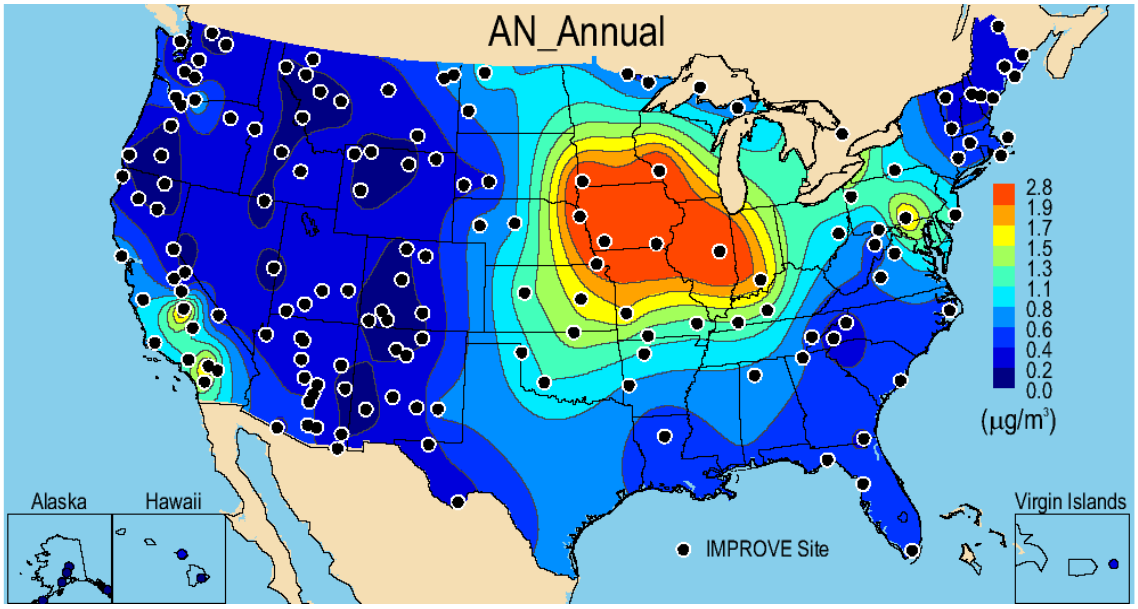

Figure 2.2.2a. IMPROVE (rural) 2005–2008 $PM_{2.5}$ ammonium nitrate (AN) annual mean mass concentrations (µg m^{-3}).

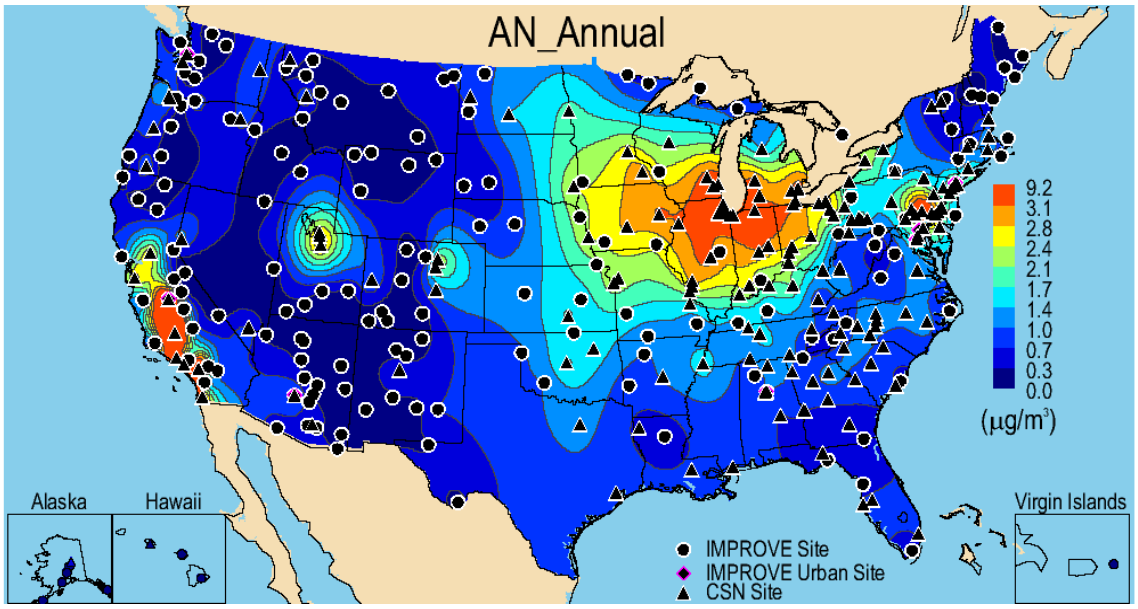

Figure 2.2.2b. IMPROVE and CSN 2005–2008 $PM_{2.5}$ ammonium nitrate (AN) annual mean mass concentrations (µg m^{-3}).

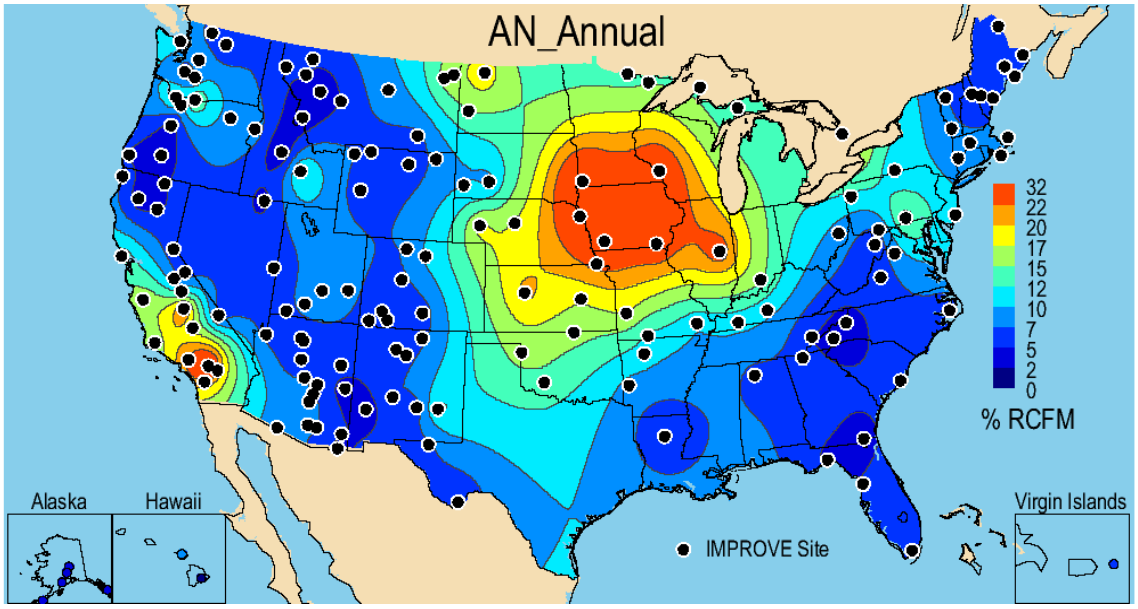

Figure 2.2.2c. IMPROVE (rural) 2005–2008 annual mean percent (%) contributions of ammonium nitrate (AN) to $PM_{2.5}$ reconstructed fine mass (RCFM).

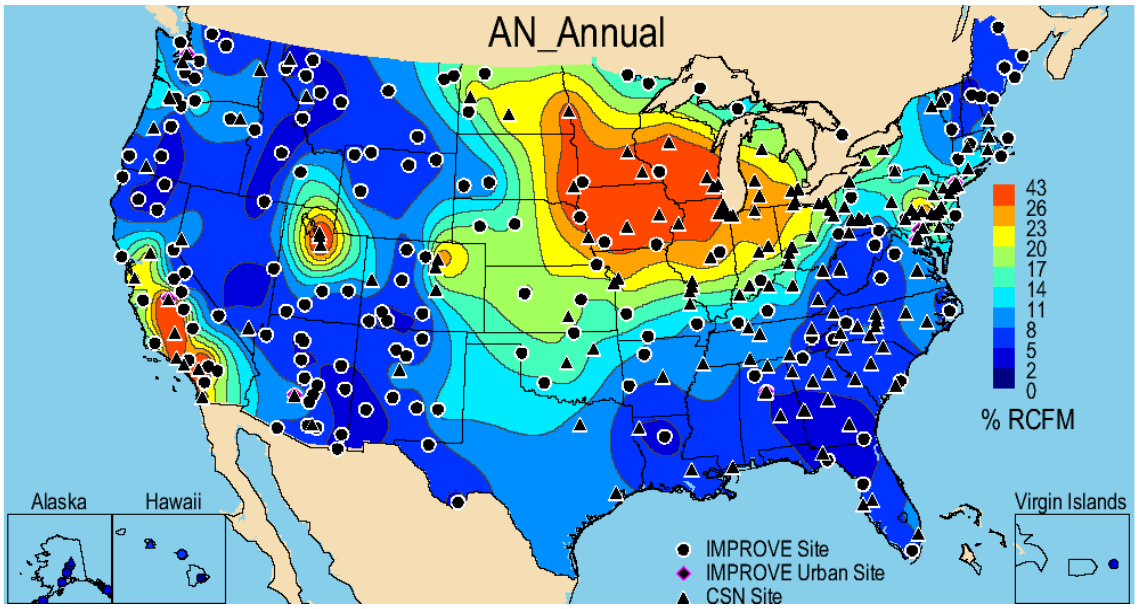

Figure 2.2.2d. IMPROVE and CSN 2005–2008 annual mean percent (%) contributions of ammonium nitrate (AN) to $PM_{2.5}$ reconstructed fine mass (RCFM).

2.2.3 $PM_{2.5}$ Particulate Organic Matter Mass

The eastern part of the United States had the highest 2005–2008 annual mean rural IMPROVE POM concentrations, with several sites in the Southeast having concentrations over 3.2 μg m^{-3} and most sites in the Northeast over 2 μg m^{-3} (Figure 2.2.3a). Elevated levels of POM in the East were most likely due to primary emissions of biomass combustion (especially in the Southeast) and secondary emissions from biogenic sources (Bench et al., 2007). The lowest concentrations occurred in the West. Concentrations in western Colorado, portions of Wyoming and New Mexico, and the Four Corners region were less than 1 μg m^{-3}. The lowest annual POM

concentration of 0.14 μg m^{-3} occurred at Haleakala Crater, Hawaii (HACR1). Portions of the Northwest and California were associated with higher concentrations. Concentrations in Idaho and Montana were near 3 μg m^{-3}, most likely from biomass burning emissions. The higher concentrations in California were associated with Trinity (TRIN1, 4.56 μg m^{-3}) and Sequoia NP (SEQU1, 3.75 μg m^{-3}). High POM concentrations were associated with urban IMPROVE sites, especially in Fresno (6.90 μg m^{-3}, FRES1) and Phoenix (4.51 μg m^{-3}, PHOE1). The urban IMPROVE site with the lowest concentration was Puget Sound (3.59 μg m^{-3}, PUSO1).

The incorporation of CSN sites in the POM spatial map resulted in higher concentrations in more focused regions, especially in the Southeast (Figure 2.2.3b). Portions of Alabama, Georgia, South Carolina, and North Carolina had POM concentrations greater than 5.5 μg m^{-3}. Urban regions along the West Coast and in the Southwest had similar patterns at the rural-only isopleths but with higher concentrations. The highest CSN concentration corresponded to a site in northwestern Montana (11.68 μg m^{-3}, Libby, #300530018), probably due to wintertime residential wood combustion as POM peaked in winter at this site (Ward et al., 2006). The maximum CSN urban POM concentration was 2.5 times higher than the maximum rural IMPROVE concentration. As in the IMPROVE network, the lowest CSN concentration occurred in Pearl City, Hawaii (0.34 μg m^{-3}, #150032004).

The areas with the highest IMPROVE POM mass fractions did not correspond to the areas with the highest POM mass concentrations, as they did for AS and AN (compare Figures 2.2.3a and 2.2.3c, for example). Many rural IMPROVE sites in the West had mass fractions higher than 54%, with the highest mass fraction of 75.1% in the rural site at Trinity, California (TRIN1) (see Figure 2.2.3c), and 79.7% at the CSN site of Libby, Montana (#300530018) (Figure 2.2.3d). Generally, in the rest of the United States the contribution of POM to RCFM was less; in fact, POM contributed less than 50% of RCFM at 86% of all IMPROVE sites and 93% of all CSN sites. In the central and eastern United States the POM contribution to RCFM was near 25–30% for both IMPROVE and CSN. However, POM was a significant contributor to RCFM at several urban CSN sites in Georgia, Alabama, and South Carolina, with contributions to RCFM greater than 40%.

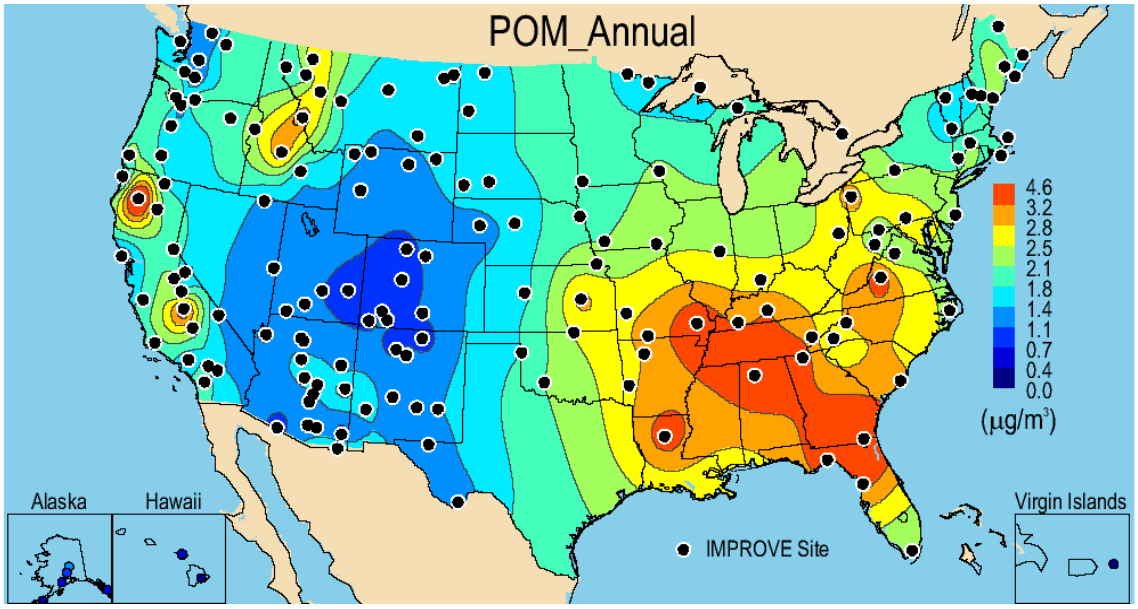

Figure 2.2.3a. IMPROVE (rural) 2005–2008 $PM_{2.5}$ particulate organic matter (POM) annual mean mass concentrations (µg m^{-3}).

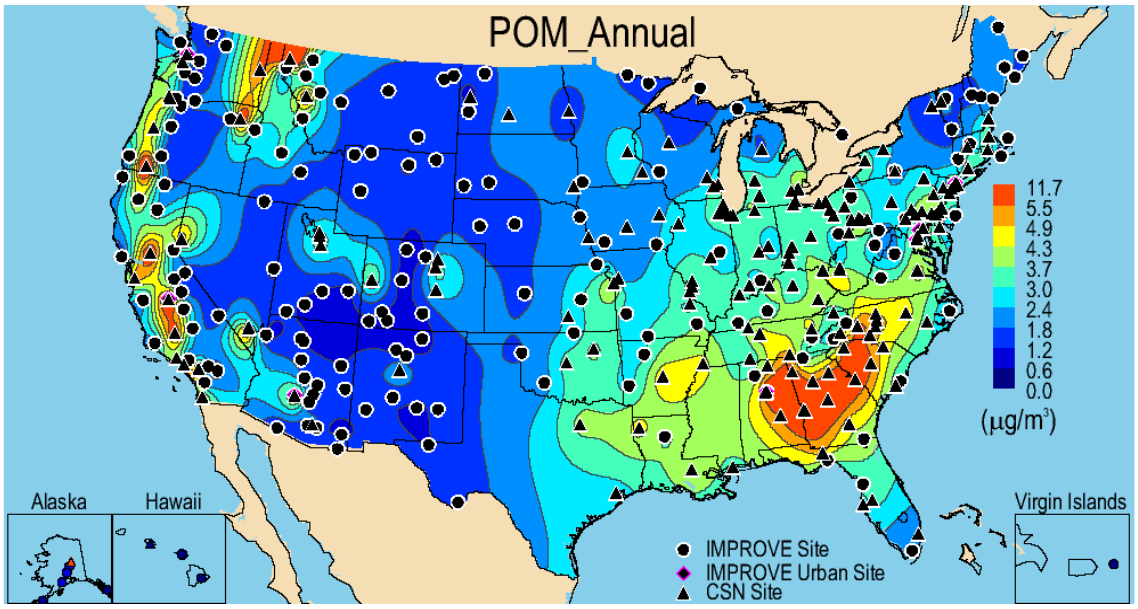

Figure 2.2.3b. IMPROVE and CSN 2005–2008 $PM_{2.5}$ particulate organic matter (POM) annual mean mass concentrations (µg m^{-3}).

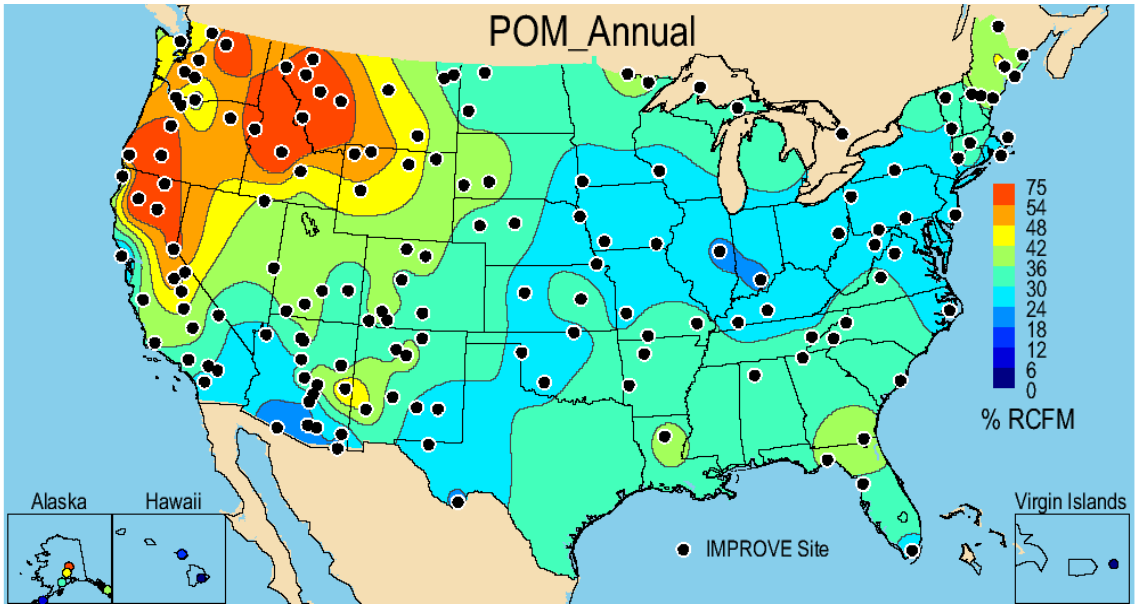

Figure 2.2.3c. IMPROVE (rural) 2005–2008 annual mean percent (%) contributions of particulate organic matter (POM) to $PM_{2.5}$ reconstructed fine mass (RCFM).

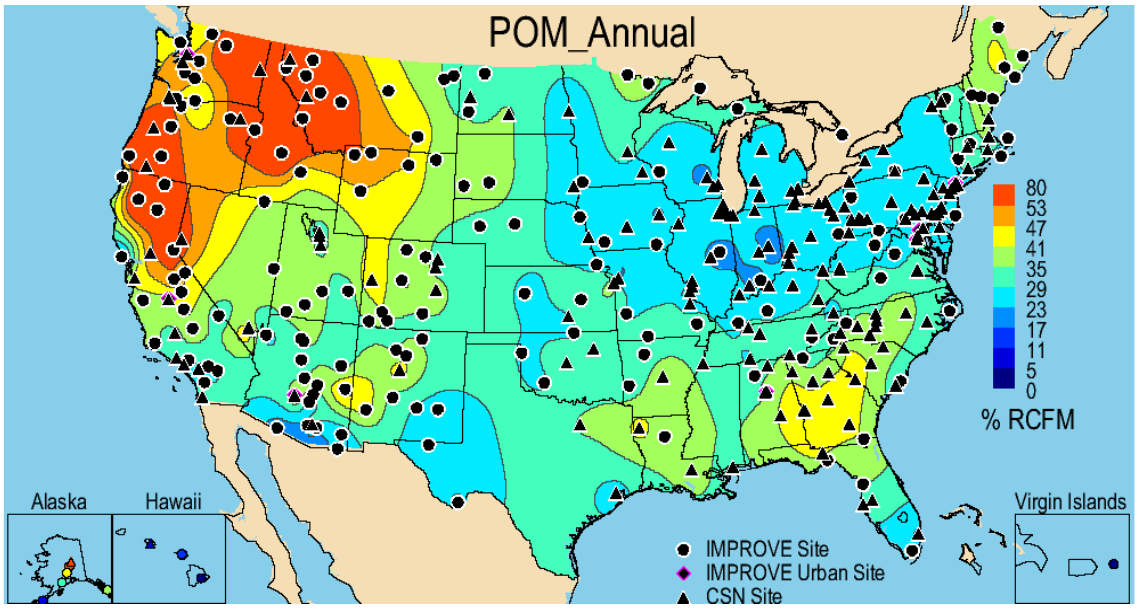

Figure 2.2.3d. IMPROVE and CSN 2005–2008 annual mean percent (%) contributions of particulate organic matter (POM) to $PM_{2.5}$ reconstructed fine mass (RCFM).

2.2.4 $PM_{2.5}$ Light Absorbing Carbon Mass

The IMPROVE rural 2005–2008 annual mean concentration ranged from 0.02 μg m^{-3} in Haleakala Crater, Hawaii (HACR1), to 0.59 μg m^{-3} in James River Face Wilderness, Virginia (JARI1). The concentrations in the West were less than 0.3 μg m^{-3}. The concentrations in the East were higher (0.4–0.5 μg m^{-3}) and tended to be located in the mid-South and Ohio River valley areas, as well as parts of Pennsylvania (Figure 2.2.4a). Major hotspots of LAC in the IMPROVE network were associated with urban sites, with the highest at Birmingham (BIRM1, 1.66 μg m^{-3}). Sites at Fresno (FRES1), Phoenix (PHOE1), Washington, D.C. (WASH1),

Baltimore (BALT1), and New York City (NEYO1) were also associated with higher concentrations (> 1 μg m^{-3}), while the lowest urban IMPROVE concentration occurred at Puget Sound (PUSO1, 0.85 μg m^{-3}).

Urban CSN concentrations were generally higher than IMPROVE (maximum of 2.58 μg m^{-3} in Liberty, Pennsylvania, #420030064, and 2.13 μg m^{-3} in Elizabeth, New Jersey, # 340390004). The spatial pattern of LAC differed from the spatial pattern of POM, suggesting different sources. For example, in the West the rural POM map showed larger regions of higher POM concentrations compared to the more localized LAC concentrations (compare Figure 2.2.3a to 2.2.4b). In addition, the urban excess noticed in the comparison of rural and urban LAC concentration maps was indicative of local urban emissions (e.g., mobile sources) of LAC rather than regional sources like biomass combustion from controlled or wild fires. The steep spatial gradient in the hotspots of LAC in the combined urban and rural map indicated that the spatial extent of the excess was small and concentrations diluted quickly before they had regional impacts (2.2.4b).

LAC is a minor contributor to RCFM at most rural sites around the United States (LAC contributed less than 5% of RCFM for 85% of rural IMPROVE sites, see Figure 2.2.4c). However, in urban regions and some northwestern sites it was as high as 7%, such as at Glacier NP in Montana (GLAC1) and Mount Rainier NP in Washington (MORA1). In the CSN urban network, LAC contributed as much as 15% (Las Vegas, #320030020) to RCFM and contributed less than 5% to RCFM for only 13% of the sites. Urban regions definitely had higher contributions from LAC in general (Figure 2.2.4d), similar to higher mass concentrations, and this influence appeared to be fairly localized.

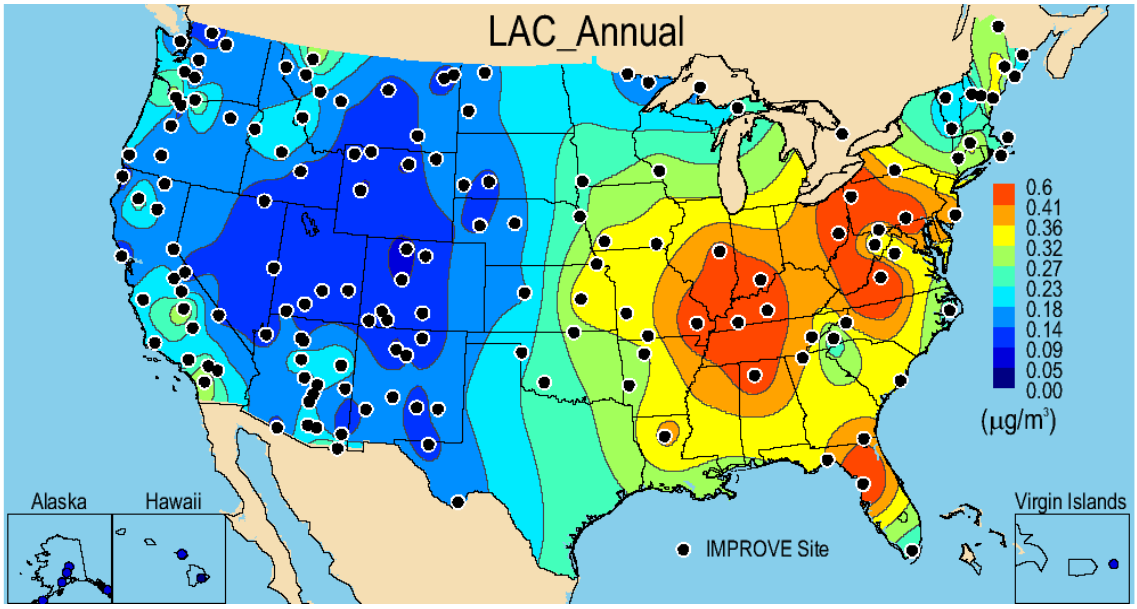

Figure 2.2.4a. IMPROVE (rural) 2005–2008 $PM_{2.5}$ light absorbing carbon (LAC) annual mean mass concentrations (μg m^{-3}).

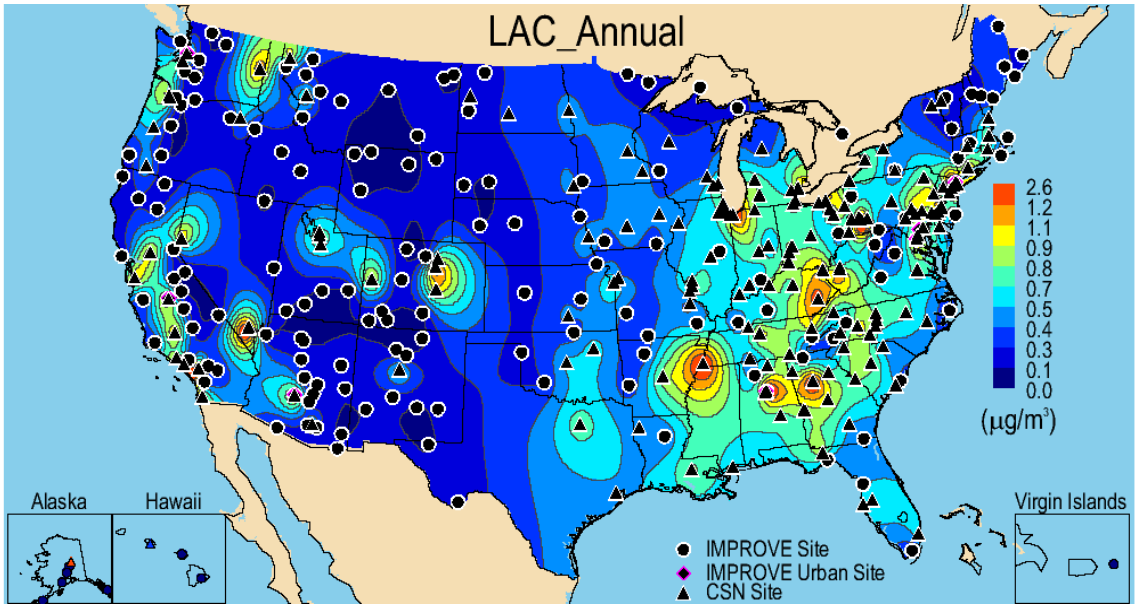

Figure 2.2.4b. IMPROVE and CSN 2005–2008 $PM_{2.5}$ light absorbing carbon (LAC) annual mean mass concentrations (μg m^{-3}).

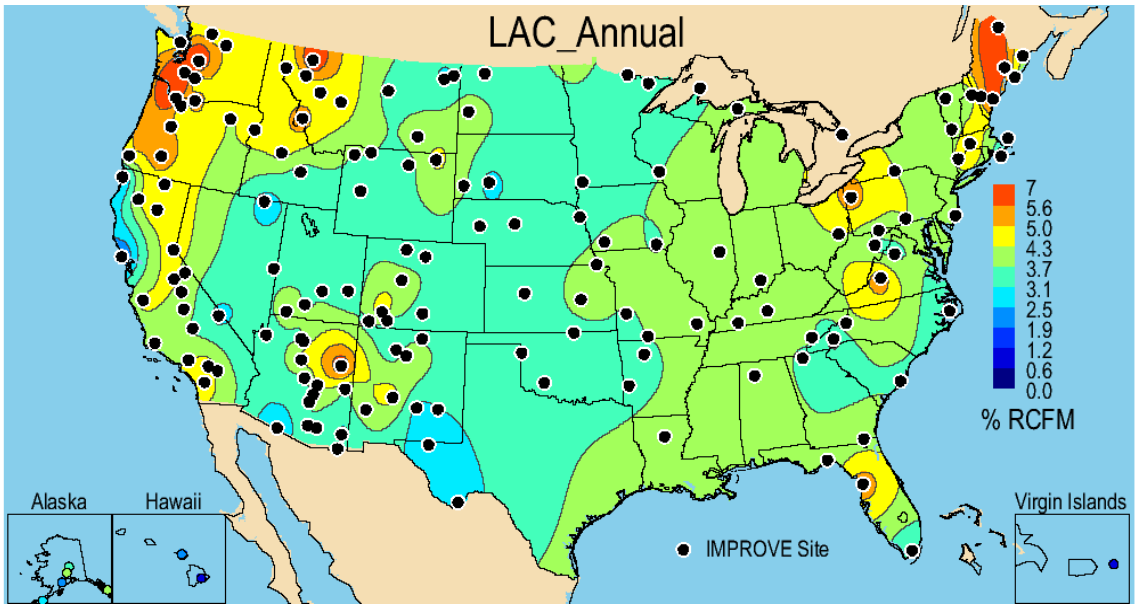

Figure 2.2.4c. IMPROVE (rural) 2005–2008 annual mean percent (%) contributions of light absorbing carbon (LAC) to $PM_{2.5}$ reconstructed fine mass (RCFM).

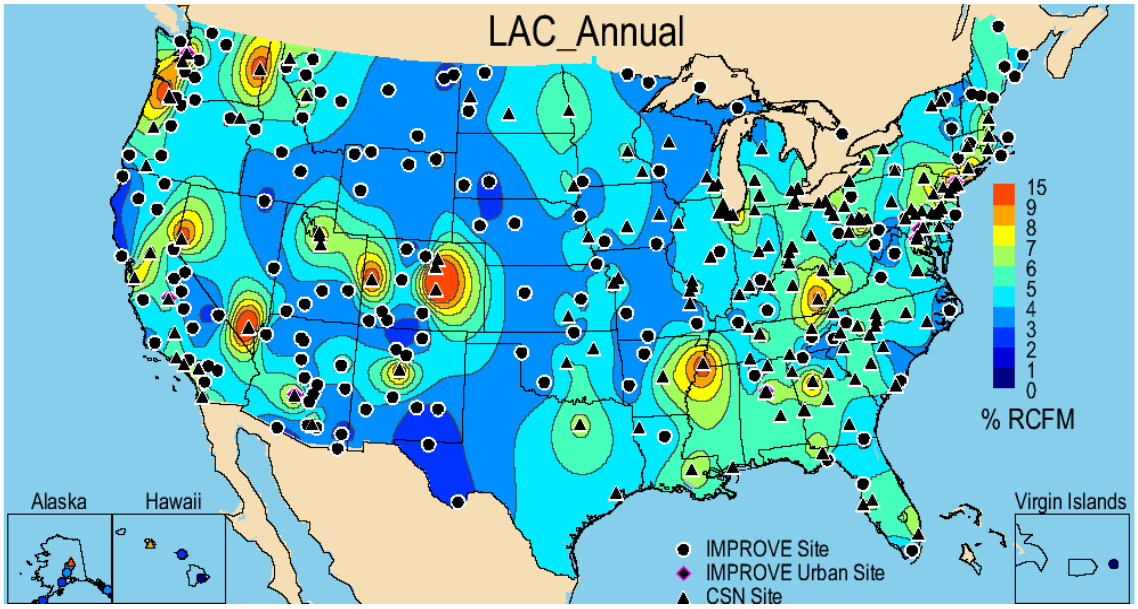

Figure 2.2.4d. IMPROVE and CSN 2005–2008 annual mean percent (%) contributions of light absorbing carbon (LAC) to $PM_{2.5}$ reconstructed fine mass (RCFM).

2.2.5 $PM_{2.5}$ Soil Mass

The patterns observed in the 2005–2008 annual mean rural IMPROVE soil concentrations were reflective of the expected transport pathways described earlier, with the exception of the Asian dust influence. The highest annual mean concentrations were in the Southwest, with the highest at Douglas, Arizona (4.41 μg m^{-3}, DOUG1). Additional sites in Arizona ranged from 1.5 to 4.4 μg m^{-3}. Sites around the Colorado Plateau and Nevada (Jarbidge, JARB1) as well as sites in southern New Mexico and west Texas had higher concentrations (> 1 μg m^{-3}, see Figure 2.2.5a). In the central United States, the highest annual mean concentration occurred at the Cherokee Nation, Oklahoma, site (1.4 μg m^{-3}, CHER1), and the urban IMPROVE site of Birmingham had the highest concentration in the South (2.0 μg m^{-3}, BIRM1). With other species the spatial patterns divided along the east/west orientation; in the case of soil the division was north/south. The concentrations at northern sites tended to be lower (~0.5 μg m^{-3}), with no "hot spots" of high soil concentration as observed in the southern regions. The minimum rural IMPROVE soil concentration occurred at Petersburg, Alaska (0.11 μg m^{-3}, PETE1). Soil is a unique case for IMPROVE, where the rural maximum concentration was higher than the urban IMPROVE maximum (3.21 μg m^{-3}, Phoenix, PHOE1). In general, adding the CSN urban sites to the spatial map did not dramatically alter the spatial pattern but did add a few urban locations where soil was more prevalent (see Figure 2.2.5b). For example, the CSN sites at Denver, Spokane, Detroit, and Rubidoux, California, corresponded to higher soil concentrations. CSN sites in the Southwest, especially Las Vegas, were also higher. The CSN Birmingham site (#10732003), which corresponded to the highest concentration for CSN (2.01 μg m^{-3}), agreed very closely with the concentration from the nearby urban IMPROVE site (BIRM1,1.99 μg m^{-3}). However, the mean soil concentration at the second CSN Birmingham site (#10730023), collocated with the urban IMPROVE sampler, was much lower (1.35 μg m-3), reflecting the relative bias reported in Table 1.9. The mean soil concentration at the collocated IMPROVE and CSN site in Birmingham was 1.35 μg m^{-3}, which was more typical of the level of agreement between IMPROVE and CSN soil concentrations reported in Table 1.9. The lowest concentration

in the CSN network was measured in northeastern New York (0.12 μg m^{-3}, Wilmington, #360310003).

Soil contributed a substantial fraction of RCFM only in the West and Southwest (Figure 2.2.5c), where contributions were typically above 25%. The highest fraction occurred at Douglas, Arizona (51.0%, DOUG1), coincident with the highest concentration. The site at Phoenix (PHOE1) corresponded to the highest fractional contribution at an urban IMPROVE site (27.3%), and Baltimore was the lowest (4.5%, BALT1). The lowest nonurban IMPROVE fractional contribution occurred at Point Reyes, California (3.2%, PORE1). Soil contributed less than 25% to the RCFM for 85% of the IMPROVE sites, along the western coast and the eastern half of the United States. The soil fraction of RCFM was less than 25% for all of the CSN urban sites (Figure 2.2.5d). The maximum fraction occurred in Las Vegas (21.8%, #320030020) and the lowest at Biglerville in south-central Pennsylvania (2.2%, #420010001).

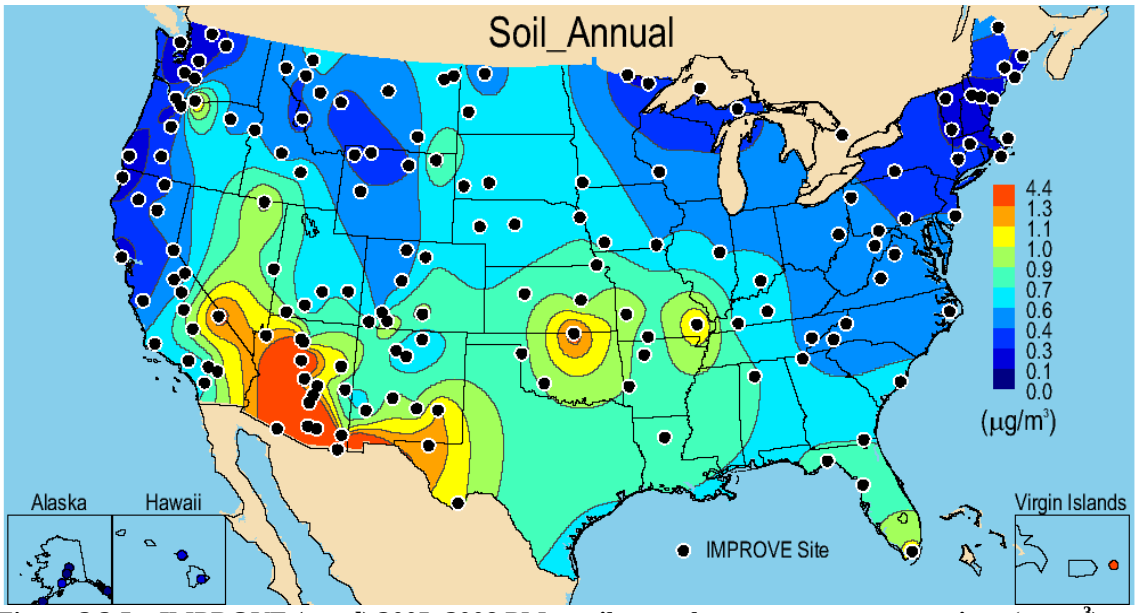

Figure 2.2.5a. IMPROVE (rural) 2005–2008 $PM_{2.5}$ soil annual mean mass concentrations (μg m^{-3}).

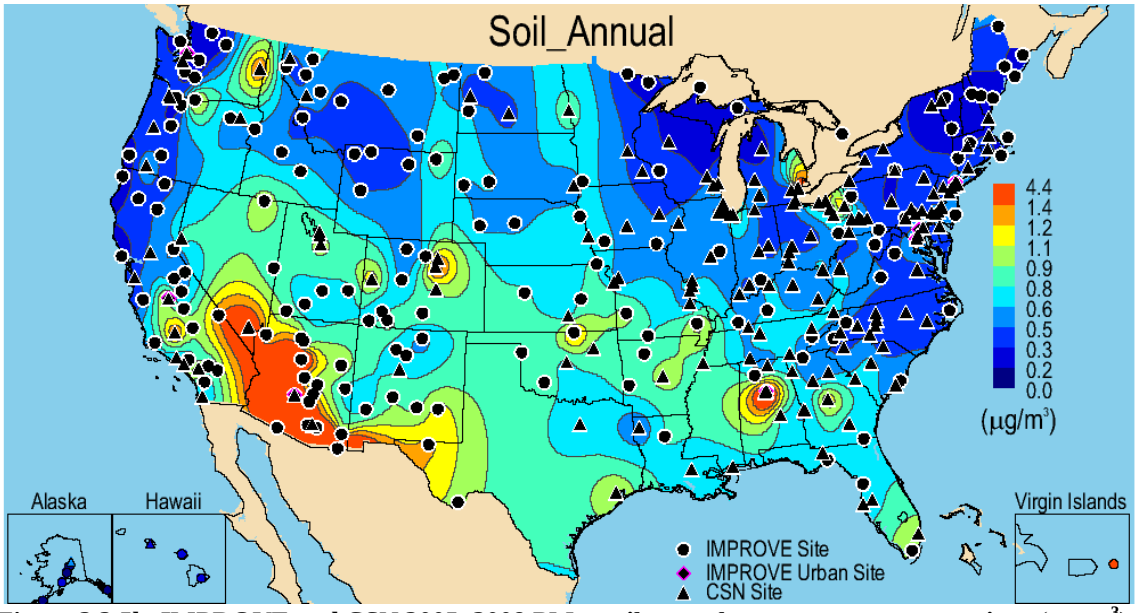

Figure 2.2.5b. IMPROVE and CSN 2005–2008 $PM_{2.5}$ soil annual mean mass concentrations (μg m^{-3}).

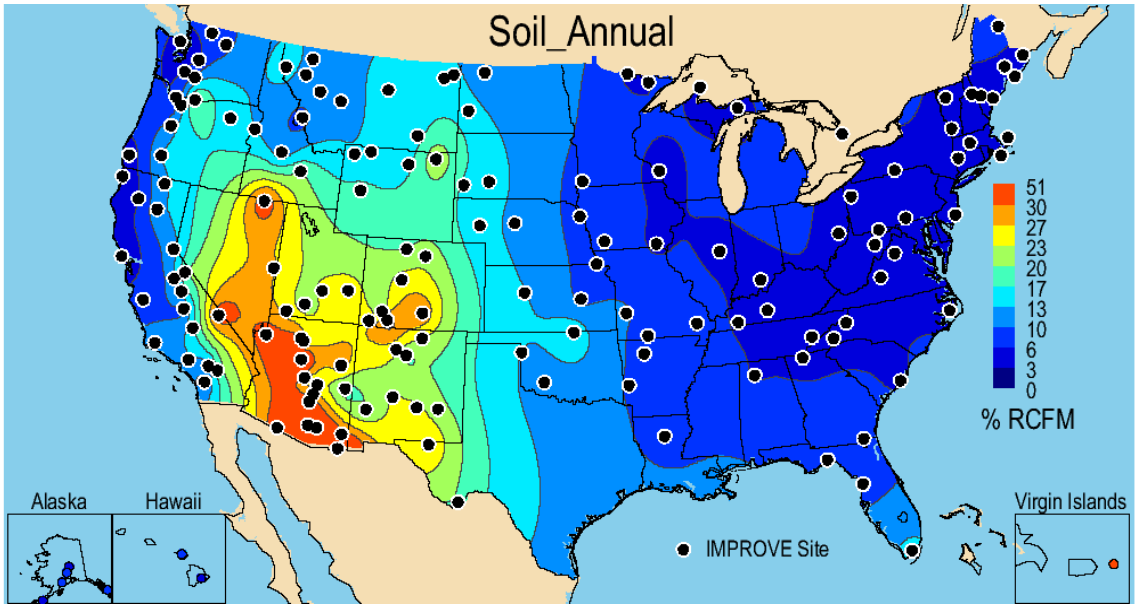

Figure 2.2.5c. IMPROVE (rural) 2005–2008 annual mean percent (%) contributions of soil to $PM_{2.5}$ reconstructed fine mass (RCFM).

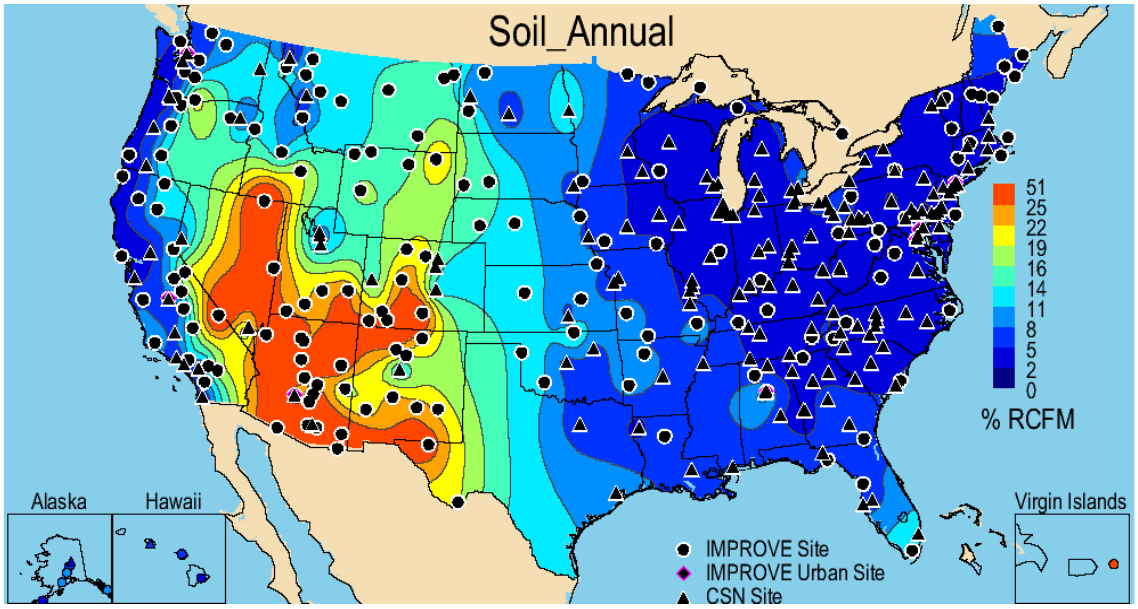

Figure 2.2.5d. IMPROVE and CSN 2005–2008 annual mean percent (%) contributions of soil to $PM_{2.5}$ reconstructed fine mass (RCFM).

2.2.6 $PM_{2.5}$ Sea Salt Mass

The IMPROVE sites with the highest 2005–2008 annual mean sea salt concentrations were, not surprisingly, at the east and west coasts (Figure 2.2.6a). Concentrations at rural IMPROVE sites ranged from 0.004 μg m^{-3} at Shamrock Mine, Colorado (SHMI1), to 2.29 μg m^{-3} at Point Reyes National Seashore, California (PORE1). On the East Coast, the site at Everglades NP in Florida (EVER1) had an annual mean concentration of 0.60 μg m^{-3}, and Cape Romain NWR in South Carolina (ROMA1) corresponded to a concentration of 0.49 μg m^{-3}. Two sites in Massachusetts had higher concentrations: Martha's Vineyard (0.84 μg m^{-3}, MAVI1) and Cape Cod (0.76 μg m^{-3}, CACO1). The Virgin Islands (VIIS) had a concentration of 1.5 μg m^{-3}. Other than these sites, the rural IMPROVE concentrations were low. The urban IMPROVE site concentrations ranged from 0.19 μg m^{-3} at Washington, D.C. (WASH1), to 0.38 μg m^{-3} at Puget Sound (PUSO1). The sea salt concentrations at CSN urban sites were typically lower than those at IMPROVE sites (Figure 2.2.6b) due to the relative biases between the two estimates (see section 1.4). The minimum concentration of 0.0013 μg m^{-3} occurred in Watford City, North Dakota (#380530002), and the maximum concentration 0f 0.97 μg m^{-3} occurred in Pearl City, Hawaii (#150032004). Nearly all of the CSN sites corresponded to concentrations that were less than 0.4 μg m^{-3}, with the exception of 0.49 μg m^{-3} in Florida (Fort Lauderdale, 120111002) and 0.56 μg m^{-3} in Pennsylvania (Liberty, #420030064) and the maximum concentration at the site in Hawaii.

At the IMPROVE site at Simeonof, Alaska (SIME1), sea salt contributed 46.1% of RCFM, compared to the minimum contribution at Shamrock Mine, Colorado (0.12%, SHMI1) (Figure 2.2.6c). At the CSN site at Pearl City, Hawaii (#150032004), sea salt contributed 26.9% of RCFM, compared to 0.04% at Watford City, North Dakota (#380530002). In general sea salt was not a major contributor to RCFM even in coastal regions; 95% of all IMPROVE sites corresponded to contributions of less than 10%, similar to 99% of all CSN sites (Figure 2.2.6d).

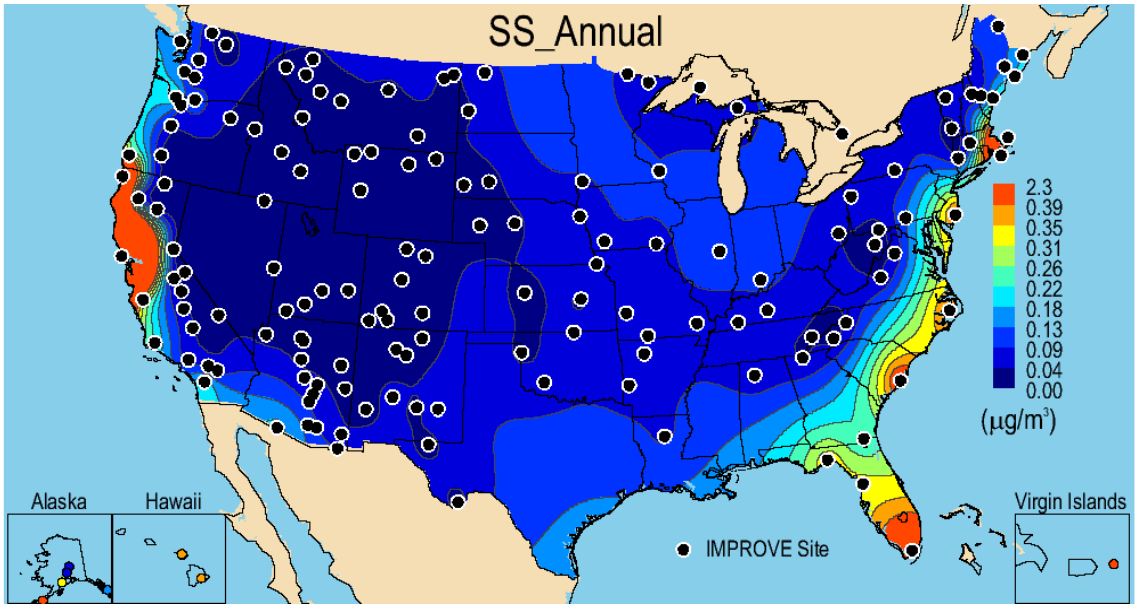

Figure 2.2.6a. IMPROVE (rural) 2005–2008 $PM_{2.5}$ sea salt (SS) annual mean mass concentrations (µg m^{-3}).

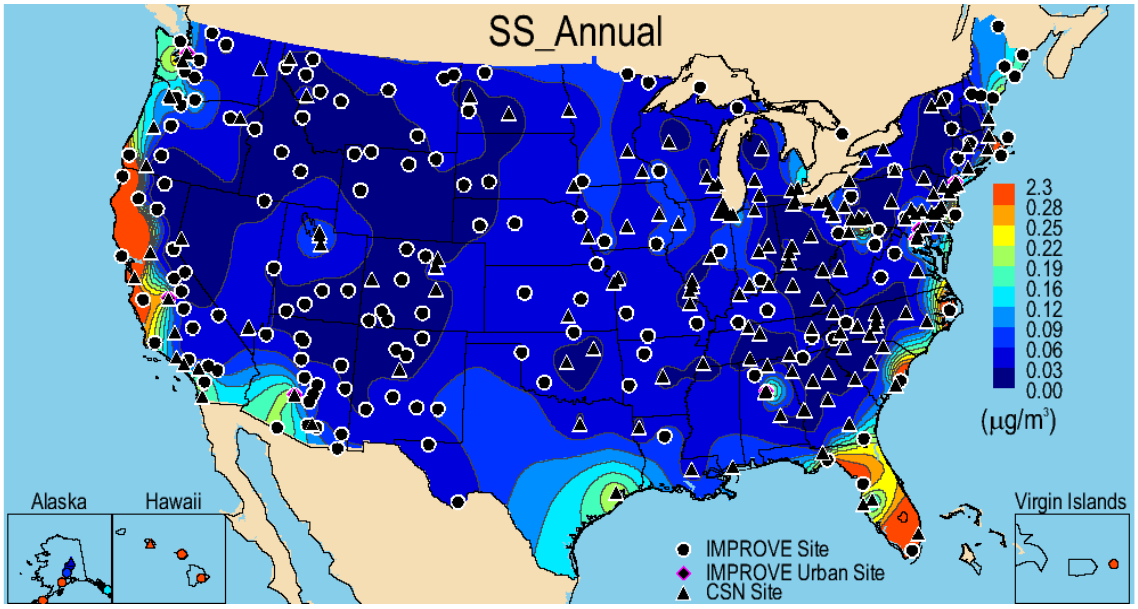

Figure 2.2.6b. IMPROVE and CSN 2005–2008 $PM_{2.5}$ sea salt (SS) annual mean mass concentrations (µg m^{-3}).

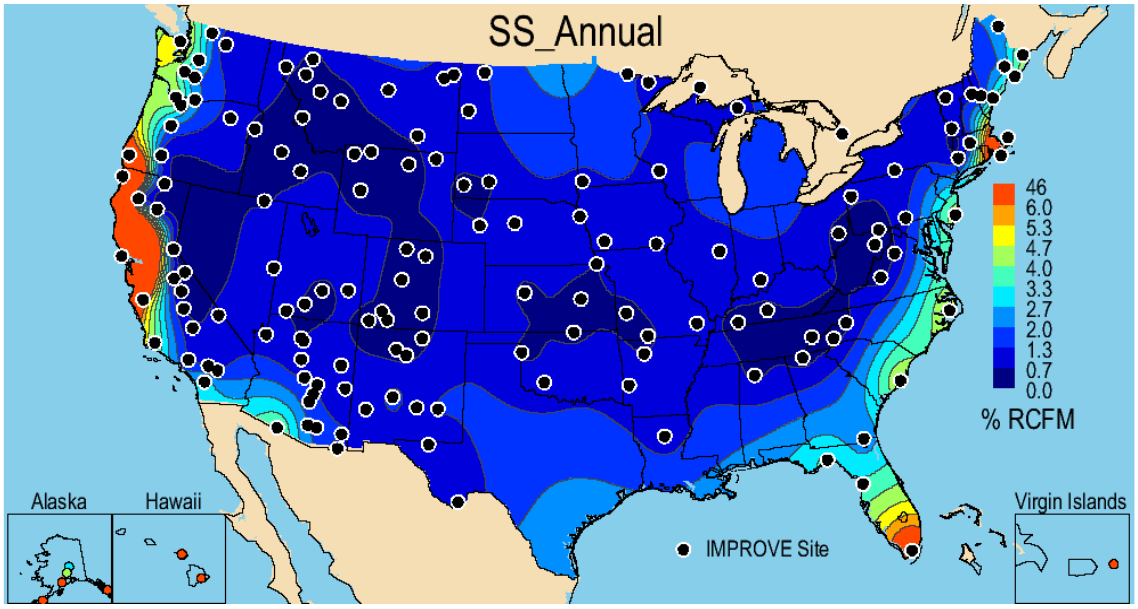

Figure 2.2.6c. IMPROVE (rural) 2005–2008 annual mean percent (%) contributions of sea salt to $PM_{2.5}$ reconstructed fine mass (RCFM).

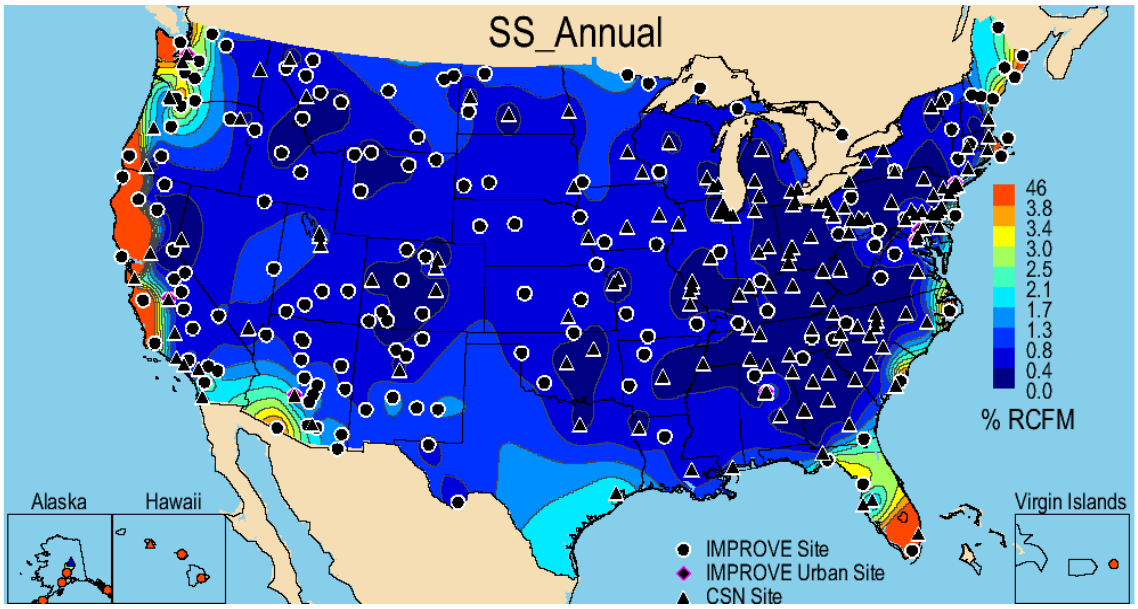

Figure 2.2.6d. IMPROVE and CSN 2005–2008 annual mean percent (%) contributions of sea salt (SS) to $PM_{2.5}$ reconstructed fine mass (RCFM).

2.2.7 $PM_{2.5}$ Gravimetric Fine Mass

The spatial pattern of 2005–2008 annual mean IMPROVE FM concentrations reflected the patterns of both the annual mean concentrations of AS, AN, and POM (compare Figure 2.2.7a to 2.2.1a, 2.2.2a, and 2.2.3a, respectively). High concentrations in the eastern United States (the maximum value of 11.67 μg m^{-3} occurred at Livonia, Indiana, LIVO1) were consistent with high concentrations of AS in this region. The western United States corresponded to lower concentrations (Figure 2.2.7a). The lowest occurred in Petersburg, Alaska (1.29 μg m^{-3}, PETE1). Two regions of higher FM concentrations in the West were associated with urban

IMPROVE sites. Phoenix (PHOE1) had an annual mean concentration of 10.27 μg m^{-3}, and Fresno (FRES1) had an FM concentration of 15.0 μg m^{-3}. The highest urban IMPROVE concentration occurred in Birmingham (17.09 μg m^{-3}, BIRM1), compared with the lowest urban concentration of 6.87 μg m^{-3} in Puget Sound (PUGO1). The urban FM concentrations measured by the CSN network were somewhat higher than the IMPROVE concentrations; only four sites had annual mean concentrations less than 6.0 μg m^{-3} (Figure 2.2.7b). The values ranged from 5.43 μg m^{-3} in Watford City, North Dakota (#380530002) to 21.48 μg m^{-3} in southwestern Pennsylvania (Liberty, #420030064). The same general pattern of high FM in the East compared to the West occurred with the addition of the CSN sites, but the impact of the urban centers, such as Denver, Salt Lake City, Rubidoux, California, Las Vegas, and Libby, Montana, was noticeable.

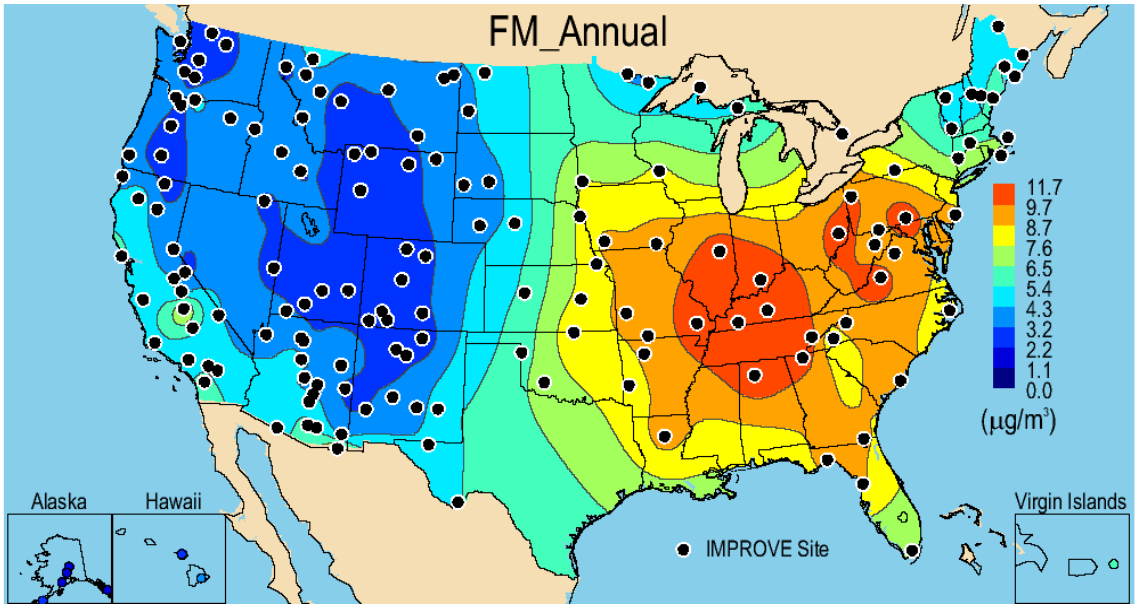

Figure 2.2.7a. IMPROVE (rural) 2005–2008 $PM_{2.5}$ annual mean gravimetric fine mass (FM) concentrations (μg m^{-3}).

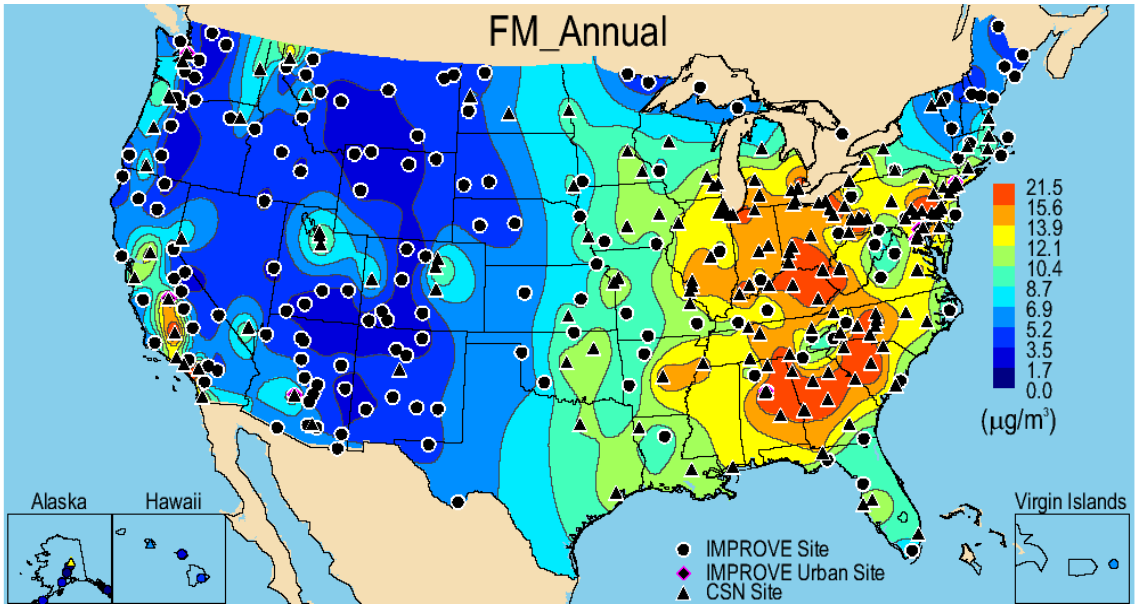

Figure 2.2.7b. IMPROVE and CSN 2005–2008 $PM_{2.5}$ annual mean gravimetric fine mass (FM) concentrations (μg m^{-3}).

2.2.8 $PM_{2.5}$ Reconstructed Fine Mass

If all of the assumptions regarding the molecular species of aerosols included in the calculation of RCFM were appropriate and there were no biases in the FM measurements, then the spatial pattern of RCFM should exactly reproduce the FM spatial pattern. Comparisons of the 2005–2008 annual mean FM and RCFM concentrations for rural IMPROVE (Figures 2.2.7a and 2.2.8a, respectively) show fairly close agreement, although there are some differences. Some of these differences in the patterns also may be due to uncertainties in the interpolation scheme. The maximum rural IMPROVE annual mean RCFM corresponded to the site at Livonia, Indiana (LIVO1, 11.73 μg m^{-3}), where the maximum AS annual mean also occurred. The minimum annual mean RCFM occurred in Petersburg, Alaska (1.18 μg m^{-3}, PETE1). The FM maximum and minimum locations occurred at the same sites, respectively.

The urban annual mean RCFM ranged between 7.77 μg m^{-3} (Puget Sound, PUSO1) and 18.17 μg m^{-3} in Fresno (FRES1), where the maximum AN annual mean also occurred. The maximum annual mean urban FM concentration occurred in Birmingham (BIRM1), not Fresno, possibly because of losses of nitrate species from the Teflon filter. The CSN annual mean RCFM concentration ranged from 3.49 μg m^{-3} at Watford City (#380530002) to 21.28 μg m^{-3} at Rubidoux (#060658001) (Figure 2.2.8b). Similarly to the IMPROVE network, the maximum CSN RCFM occurred at the same location as the maximum AN. Further investigation into the differences between FM and RCFM will be presented in the next section.

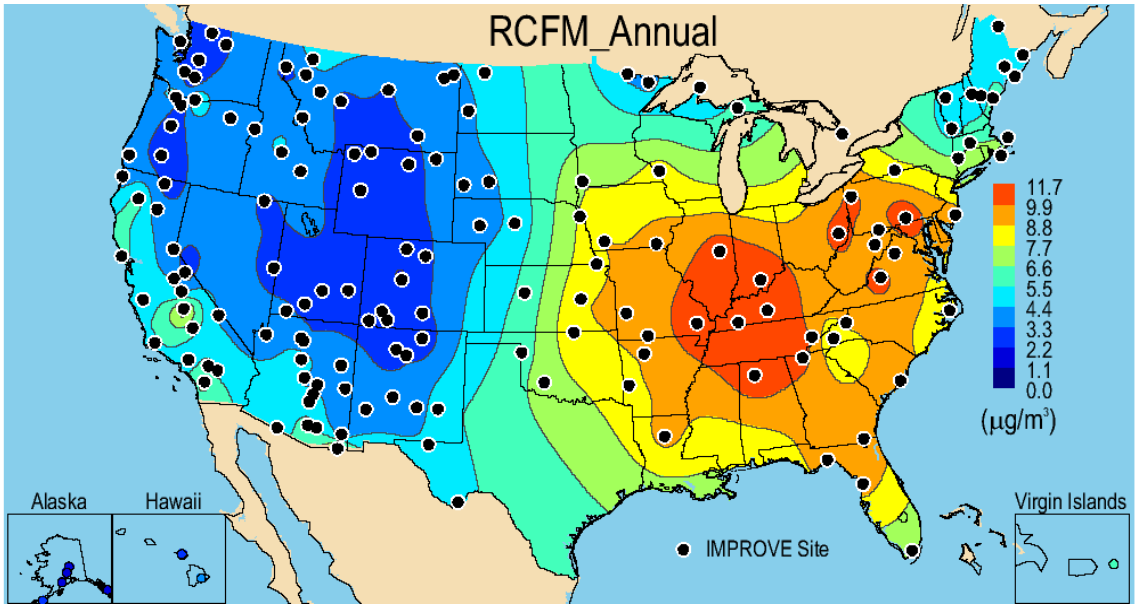

Figure 2.2.8a. IMPROVE (rural) 2005–2008 $PM_{2.5}$ annual mean reconstructed fine mass (RCFM) concentrations (µg m^{-3}).

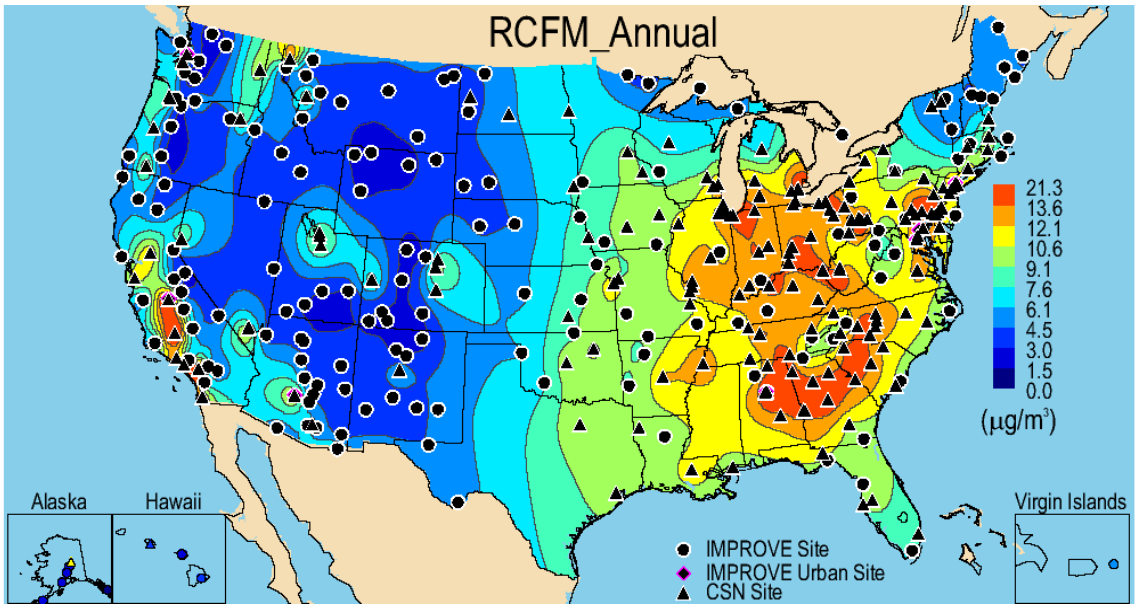

Figure 2.2.8.b. IMPROVE and CSN 2005–2008 $PM_{2.5}$ annual mean reconstructed fine mass (RCFM) concentrations (µg m^{-3}).

2.2.9 Differences in $PM_{2.5}$ Gravimetric and Reconstructed Fine Mass

Differences between 2005−2008 annual mean FM and RCFM (dM = FM - RCFM) for most of the rural IMPROVE sites were fairly low (Figure 2.2.9a). The rural mass difference ranged from -1.14 at Okefenokee, Georgia (OKEF1) to 0.6 µg m^{-3} at Linville Gorge, North Carolina (LIGO1). RCFM overestimated FM (negative dM) at many rural IMPROVE sites and all of the urban IMPROVE sites. The largest overestimate occurred at Fresno (-3.18 µg m^{-3}), most likely due to a loss of nitrate on the fine mass Teflon filter. An inappropriately-high R_{oc} factor may also have contributed. The usual east/west differences in the spatial patterns of dM

were not observed with the IMPROVE rural sites, but this division was more obvious with the addition of urban CSN sites (Figure 2.2.9b). In contrast to the IMPROVE sites, RCFM underestimated FM concentrations at most of the CSN urban sites. The mass difference ranged from -1.37 μg m^{-3} at Los Angeles (#060371103) to 5.25 μg m^{-3} at Columbia, South Carolina (#450790019). For 35% of CSN sites, RCFM was underestimated by more than 2 μg m^{-3}. Sites in the East corresponded to the highest dM. An examination of values of dM at collocated urban IMPROVE and CSN sites revealed negative IMPROVE dM values contrasting positive CSN dM values at the same site. The discrepancy arose from higher CSN FM concentrations compared to IMPROVE FM concentrations (recall the relative biases of 0.04% and 18.4% in RCFM and FM, respectively, reported in Table 1.9). Higher CSN FM concentrations were most likely associated with smaller negative sampling artifacts due to lower filter face velocities of CSN samplers compared with the IMPROVE sampler. Adjusting the CSN OC data to agree with IMPROVE OC data introduced an inconsistency between the CSN RCFM and FM by reducing RCFM concentrations that otherwise would have been consistent with higher FM values. Further investigation of biases associated with FM measurements will be explored in Chapter 8 (Malm et al., 2011).

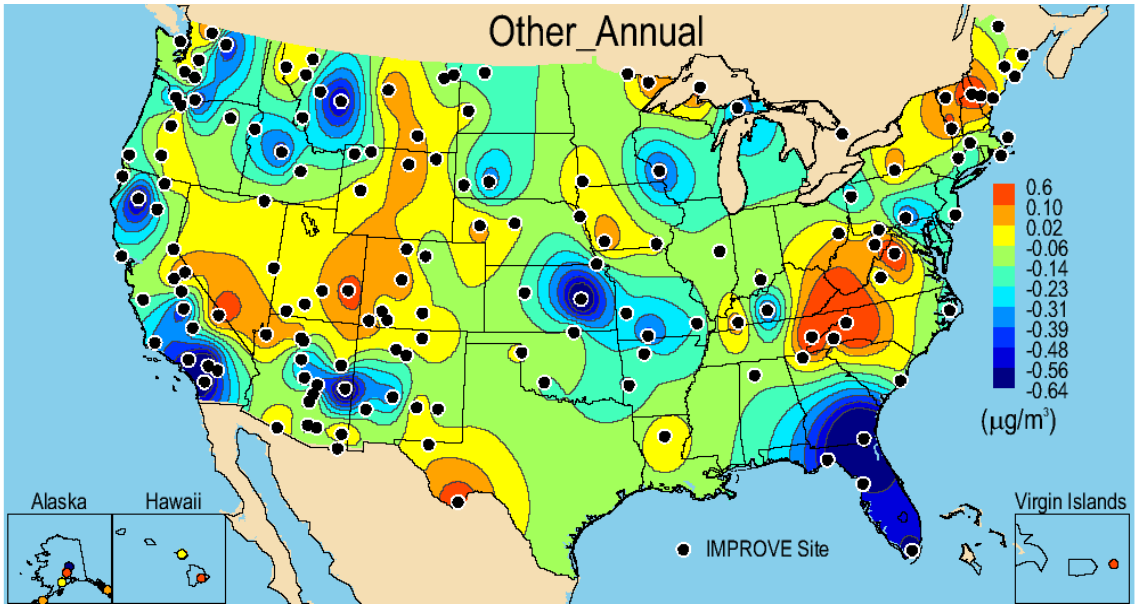

Figure 2.2.9a. IMPROVE (rural) 2005–2008 $PM_{2.5}$ annual mean mass difference (dM = FM - RCFM) between $PM_{2.5}$ gravimetric fine mass (FM) and reconstructed fine mass (RCFM) (μg m^{-3}).

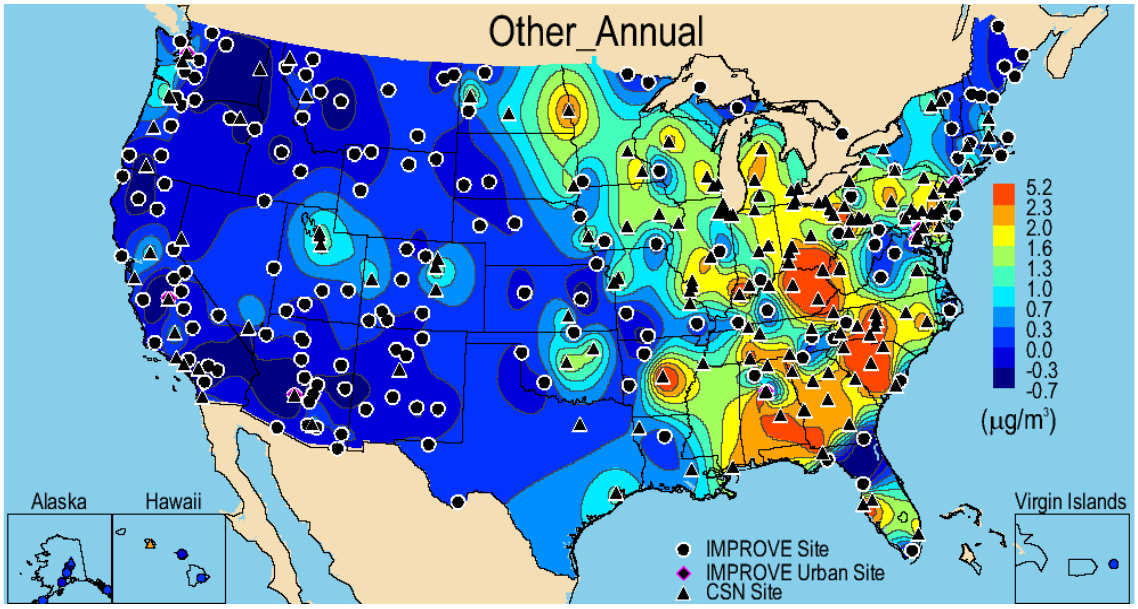

Figure 2.2.9b. IMPROVE and CSN 2005–2008 $PM_{2.5}$ annual mean difference (dM = FM - RCFM) between $PM_{2.5}$ gravimetric fine mass (FM) and reconstructed fine mass (RCFM) (µg m^{-3}).

2.2.10 Coarse Mass

Coarse mass (CM) data were only available for the IMPROVE network and were derived from the difference in PM_{10} and $PM_{2.5}$ gravimetric mass concentrations. The rural CM 2005−2008 annual mean concentration ranged from 1.12 µg m^{-3} in North Cascades, Washington (NOCA1), to 21.12 µg m^{-3} in Douglas, Arizona (DOUG1) (Figure 2.2.10). The high concentration in Douglas was most likely associated with mineral dust. In fact, high concentrations at several sites in the Southwest were observed, similar to soil concentrations (see Figure 2.2.5a). The urban IMPROVE CM ranged from 6.42 µg m^{-3} in Baltimore (BALT1) to 20.51 µg m^{-3} in Phoenix (PHOE1). Twelve sites corresponded to CM greater than 10 µg m^{-3}. With the exception of New York City (NEYO1) and Puget Sound (PUSO1), all of the IMPROVE urban sites had high concentrations (CM > 10 µg m^{-3}). In the central United States higher concentrations most likely corresponded to agricultural activity and fugitive dust (Malm et al., 2007). The annual mean concentration at Cherokee Nation, Oklahoma (CHER1), was 15.70 µg m^{-3}, Mingo, Missouri, had a concentration of 9.02 µg m^{-3} (MING1), and Viking Lake, Iowa, (VILA1) had a concentration of 9.41 µg m^{-3}. Comparisons of annual mean $PM_{2.5}$ soil and CM concentration spatial maps suggested that species other than soil were contributing to CM, especially in the central states. Sites in Iowa and Missouri had high CM concentrations but not necessarily high soil concentrations. In contrast, sites in southern Arizona corresponded to both high fine soil and CM, as would be expected if CM was predominantly soil. High concentrations of CM were also observed at the Virgin Islands site (12.06 µg m^{-3}), probably due to dust and/or sea salt. Lower concentrations were observed along the Appalachian region and in the Northeast, the Rocky Mountain region, the Northwest (with the exception of the Columbia River Gorge, Washington), and northern California.

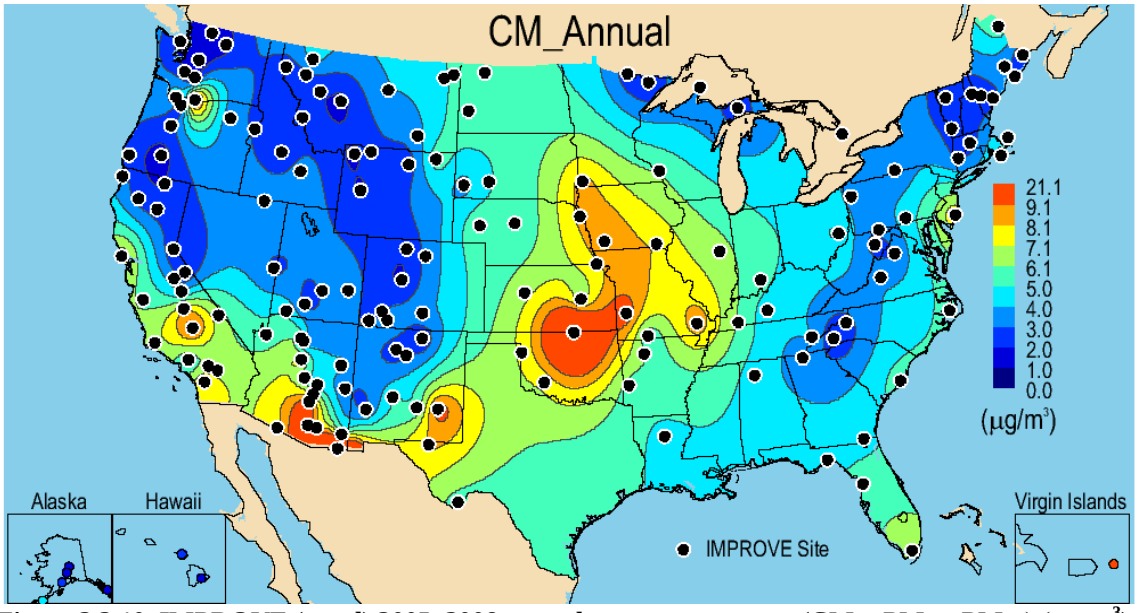

Figure 2.2.10. IMPROVE (rural) 2005–2008 annual mean coarse mass (CM = PM_{10} - $PM_{2.5}$) (µg m^{-3}).

2.2.10 PM_{10} Mass

The spatial pattern of 2005–2008 annual mean rural IMPROVE annual mean PM_{10} mass concentrations reflected the combined CM and FM spatial patterns. The regions of higher PM_{10} concentrations included the eastern half of the United States where $PM_{2.5}$ concentrations were high but also included regions in the Midwest where high CM concentrations were high (Figure 2.2.11a). Sites along the western coast and in the Southwest and California were also associated with high PM_{10} concentrations. The annual mean IMPROVE PM_{10} concentrations ranged from 2.47 µg m^{-3} in Petersburg, Alaska (PETE1), to 29.47 µg m^{-3} in Douglas, Arizona (DOUG1). The high annual mean concentration in Douglas was primarily associated with soil. IMPROVE urban concentrations of PM_{10} were higher than rural concentrations. The urban IMPROVE PM_{10} concentrations ranged from 13.28 µg m^{-3} in Puget Sound (PUSO1) to 34.94 µg m^{-3} in Fresno (FRES1). The site at Fresno also corresponded to high CM as discussed previously. Unfortunately, we have no speciated CM data for Fresno to comment on the major species contributing to CM at that site. The EPA PM_{10} mass concentration spatial map demonstrated much higher spatial variability compared to the IMPROVE data (Figure 2.2.11b). No large regional impacts were observed, with perhaps an exception in the Southwest. Several "hot spots" occurred around the country, with the highest concentration areas in California and the Southwest. The PM_{10} concentrations were also much higher at the EPA sites, suggesting local sources with high spatial variability. The PM_{10} annual mean concentrations ranged from 6.07 µg m^{-3} in Lava Beds National Monument, California (#060930005), to 86.38 µg m^{-3} near Mono Lake, also in California (#060510011). The Mono Lake site location is associated with significant dust emissions from dry lake beds and often has been in nonattainment of EPA air quality standards (e.g., GBUAPCD, 2010). EPA PM_{10} sites are located in both rural and urban locations, and the lack of regional spatial patterns demonstrates the high degree in spatial variability and fairly local impact of many PM_{10} sources.

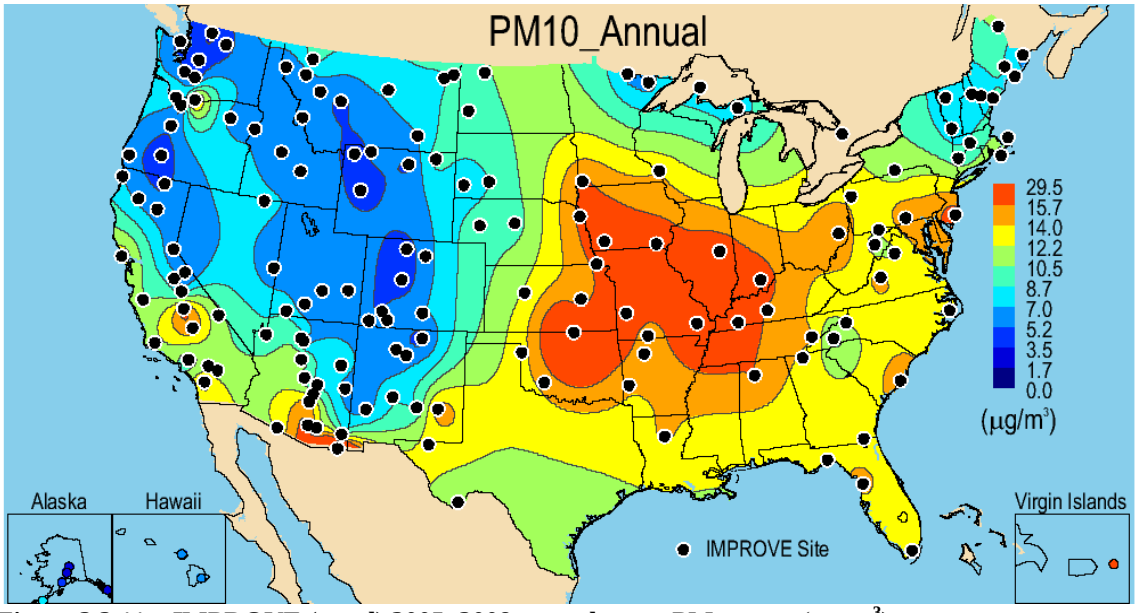

Figure 2.2.11a. IMPROVE (rural) 2005–2008 annual mean PM_{10} mass (µg m^{-3}).

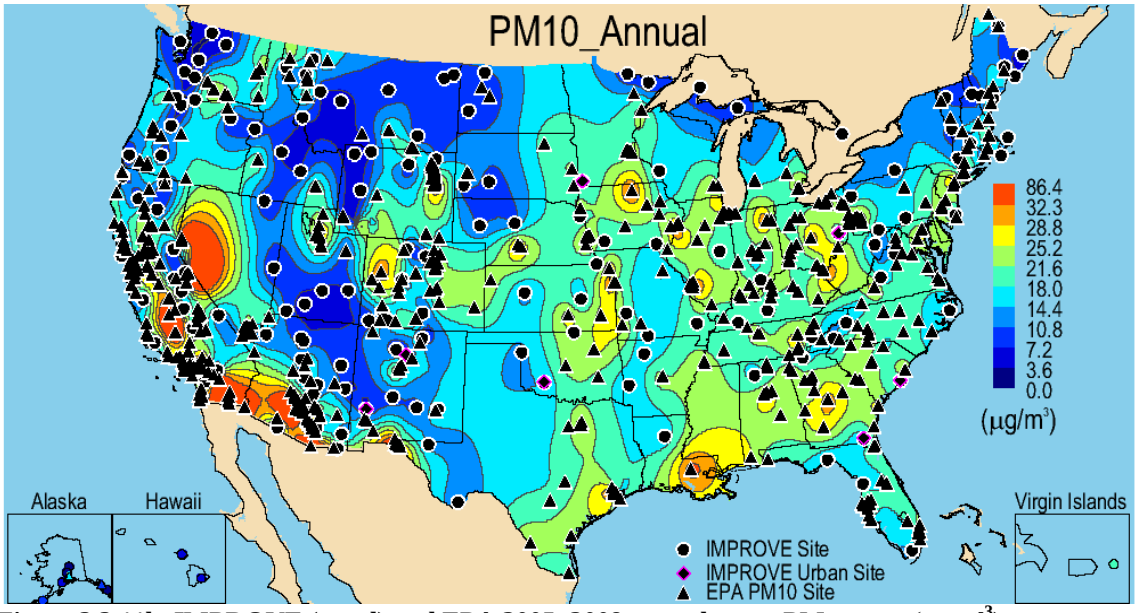

Figure 2.2.11b. IMPROVE (rural) and EPA 2005–2008 annual mean PM_{10} mass (µg m^{-3}).

REFERENCES

Ashbaugh, L. L., and R. A. Eldred (2004), Loss of particle nitrate from Teflon sampling filters: Effects on measured gravimetric mass in California and in the IMPROVE network, *J. Air Waste Manage., 54*, 93-104.

Barna, M. G., K. A. Gebhart, B. A. Schichtel, and W. C. Malm (2006), Modeling regional sulfate during the BRAVO study: Part 1. Base emissions simulation and performance evaluation, *Atmos. Environ. 40*, 2436-2448.

Bench, G., S. Fallon, B. Schichtel, W. Malm, and C. McDade (2007), Relative contributions of fossil and contemporary carbon sources to $PM_{2.5}$ aerosol in nine Interagency Monitoring for Protected Visual Environments (IMPROVE) network sites, *J. Geophys. Res., 112,* D10205, doi:10.1029/2006JD007708.

Bond, T. C., and R. W. Bergstrom (2006), Light absorption by carbonaceous particles: An investigative review, *Aerosol. Sci. Technol.*, 40(1), 27-67.

Chow, J. C., J. G. Watson, L. C. Pritchett, W. R. Pierson, C. A. Frazier, and R. G. Purcell (1993), The DRI thermal/optical reflectance carbon analysis system: Description, evaluation and applications in U.S. air quality studies, *Atmos. Env., 27A(8),* 1185-1201.

Countess, R. J., G. T. Wolff, and S. H. Cadle (1980), The Denver winter aerosol: A comprehensive chemical characterization, *J. Air Pollution Control Assoc., 30,* 1194-1200.

Chu, S.-H. (2004), $PM_{2.5}$ episodes as observed in the speciation trends network, *Atmos. Environ., 38,* 5237-5246.

Day, D. E., W. C. Malm, and S. M. Kreidenweis (1997), Seasonal variations in aerosol composition and acidity at Shenandoah and Great Smoky Mountains national parks, *J. Air Waste Manage., 47,* 411-418.

Debell, L. J., K. Gebhart, J. L. Hand, W. C. Malm, M. L. Pitchford, B. A. Schichtel, and W. H. White (2006), IMPROVE (Interagency Monitoring of Protected Visual Environments): Spatial and seasonal patterns and temporal variability of haze and its constituents in the United States: Report IV, CIRA Report ISSN: 0737-5352-74, Colo. State Univ., Fort Collins.

Eldred, B. (2002), Carbon artifact on Version 2 IMPROVE Samplers, Doc. # 004, (http://vista.cira.colostate.edu/improve/Publications/GrayLit/004_Quartz_Blanks/004_quartz_blanks.htm).

El-Zanan, H. S., D. H. Lowenthal, B. Zielinska, J. C. Chow, and N. Kumar (2005), Determination of the organic aerosol mass to organic carbon ratio in IMPROVE samples, *Chemosphere, 60(4),* 485-496.

Frank, N. H. (2006), Retained nitrate, hydrated sulfates, and carbonaceous mass in Federal Reference Method fine particulate matter for six eastern U.S. cities, *J. Air & Waste Manage. Assoc., 56,* 500-511.

GBUAPCD (2010), Reasonable further progress report for the Mono Basin PM-10 state implementation plan, http://www.gbuapcd.org/Air%20Quality%20Plans/MONO-SIP/MonoBasinReasonableFurtherProgressReport2010.pdf.

Gebhart, K. A., W. C. Malm, and D. E. Day (1994), Examination of the effects of sulfate acidity and relative humidity on light scattering at Shenandoah National Park, *Atmos. Environ., 28(5),* 841-849.

Gebhart K. A., B. A. Schichtel, M. G. Barna, and W. C. Malm (2006), Quantitative back-trajectory apportionment of sources of particulate sulfate at Big Bend National Park TX, *Atmos. Environ., 40,* 2823-2834.

Grosjean, D., and S. K. Friedlander (1975), Gas-particle distribution factors for organics and other pollutants in the Los Angeles atmosphere, *J. Air Pollution Control Assoc., 25,* 1038-1044.

Hand, J. L. (2001), A new technique for obtaining aerosol size distributions with applications to estimates of aerosol properties, Ph.D. Dissertation, Colorado State University.

Hand, J. L., and S. M. Kreidenweis (2002), A new method for retrieving particle refractive index and effective density from aerosol size distribution data, *Aerosol Sci. Technol., 36,* 1012-1026.

Hand, J. L., S. M. Kreidenweis, D. E. Sherman, J. L. Collett, Jr., S. V. Hering, D. E. Day, W. C. Malm (2002), Aerosol size distributions and visibility estimates during the Big Bend Regional Aerosol Visibility and Observational Study (BRAVO), *Atmos. Environ., 36,* 5043-5055.

Hand, J. L., W. C. Malm, A. Laskin, D. Day, T. Lee, C. Wang, C. Carrico, J. Carrillo, J. P. Cowin, J. Collett, Jr., and M. J. Iedema (2005), Optical, physical, and chemical properties of tar balls observed during the Yosemite Aerosol Characterization Study, *J. Geophys. Res., 110,* D21210, doi:10.1029/2004JD005728.

Hand, J. L., and W. C. Malm (2006), Review of the IMPROVE equation for estimating ambient light extinction coefficients, CIRA Report, ISSN: 0737-5352-71, Colo. State Univ., Fort Collins.

Hering, S., and G. Cass (1999), The magnitude of bias in the measurement of $PM_{2.5}$ arising from volatilization of particulate nitrate from Teflon filters, *J. Air Waste Manage., 49,* 725-733.

Hogrefe O., J. J. Schwab, F. Drewnick, G. G. Lala, S. Peters, K. J. Demerjian, K. Rhoads, H. D. Felton, O. V. Rattigan, L. Husain, and V. A. Dutkiewicz (2004), Semicontinuous $PM_{2.5}$ sulfate and nitrate measurements at an urban and rural location in New York: PMTACS-NY summer 2001 and 2002 campaigns, *J. Air Waste Manage., 54,* 1040-1060.

Husar, R. B., D. M. Tratt, B. A. Schichtel, S. R. Falke, F. Li, D. Jaffe, S. Gasso, T. Gill, N. S. Laulainen, F. Lu, M. C. Reheis, Y. Chun, D. Westphal, B. N. Holben, C. Gueymard, I. McKendry, N. Kuring, G. C. Feldman, C. McClain, R. J. Frouin, J. Merrill, D. DuBois, F. Vignola, T. Murayama, S. Nickovic, W. E. Wilson, K. Sassen, N. Sugimoto, and W. C. Malm (2001), Asian dust events of April, 1998, *J. Geophys. Res., 106,* D16, 18317-18330.

Jaffe, D., J. Snow, and O. Cooper (2003), The April 2001 Asian dust events: Transport and substantial impact on surface particulate matter concentrations across the United States, *Eos, Transactions,* November 18.

Japar, S. M., A. C. Szkarlat, R. A. Gorse, Jr., E. K. Heyerdahl, R. L. Johnson, J. A. Rau, and J. J. Huntzicker (1984), Comparison of solvent extraction and thermal optical carbon analysis methods: Application to diesel vehicle exhaust aerosol, *Environ. Sci. Techonol., 18,* 231-234.

Lee, T., X.-Y. Yu, B. Ayers, S. M. Kreidenweis, W. C. Malm, and J. L. Collett, Jr. (2008), Observations of fine and coarse particle nitrate at several rural locations in the United States, *Atmos. Environ.,42,* 2720-2732.

Lefer, B. L., and R. W. Talbot (2001), Summertime measurements of aerosol nitrate and ammonium at a northeastern U.S. site, *J. Geophys. Res., 106(D17),* 20365-20378.

Liu L.-J. S., R. Burton, W. E. Wilson, and P. Koutrakis (1996), Comparison of aerosol acidity in urban and semi-rural environments, *Atmos. Environ., 30*(8), 1237-1245.

Lowenthal, D. H., J. G. Watson, P. Saxena (2000), Contributions to light extinction during project MOHAVE, *Atmos. Environ., 34,* 2351-2359.

Malm, W. C., J. F. Sisler, D. Huffman, R. A. Eldred, and T. A. Cahill (1994), Spatial and seasonal trends in particle concentration and optical extinction in the United States, *J. Geophys. Res., 99(D1),* 1347-1370.

Malm, W. C., and J. L. Hand (2007), An examination of the physical and optical properties of aerosols collected in the IMPROVE program, *Atmos. Environ., 41,* 3407-3427.

Malm, W. C., M. L. Pitchford, C. McDade, and L. L. Ashbaugh (2007), Coarse particle speciation at selected locations in the rural continental United States, *Atmos. Environ., 41,* 2225-2239.

Malm, W. C., B. A. Schichtel, and M. L. Pitchford (2011), Uncertainties in $PM_{2.5}$ gravimetric and speciation measurements and what we can learn from them, *J. Air Waste Manage,* In press.

Prospero, J. M., P. Ginoux, O. Torres, S. E. Nicholson, and T. E. Gill (2002), Environmental characterization of global sources of atmospheric soil dust identified with the NIMBUS 7 Total Ozone Mapping Spectrometer (TOMS) absorbing aerosol product, *Reviews of Geophysics, 40,* 1-31.

Perry, K. D., T. A. Cahill, R. A. Eldred, and D. D. Dutcher (1997), Long-range transport of North African dust to the eastern United States, *J. Geophys. Res., 102(D10),* 11225-11238.

Quinn, P. K., D. J. Coffman, T. S. Bates, T. L. Miller, J. E. Johnson, K. Voss, E. J. Welton, and C. Neususs (2001), Dominant aerosol chemical components and their contribution to extinction during the Aerosols99 cruise across the Atlantic, *J. Geophys. Res., 106(D18),* 20783-20809.

Quinn, P.K., T. L. Miller, T. S. Bates, J. A. Ogren, E. Andrews, and G. E. Shaw (2002a), A 3-year record of simultaneously measured aerosol chemical and optical properties at Barrow, Alaska, *J. Geophys. Res., 107(D11),* 4130, 10:1029/2001JD001248.

Quinn, P. K., D. J. Coffman, T. S. Bates, T. L. Miller, J. E. Johnson, E. J. Welton, C. Neususs, M. Miller, and P. J. Sheridan (2002b), Aerosol optical properties during INDOEX 1999: Means, variability, and controlling factors, *J. Geophys. Res., 107(D19),* 8020, doi:10.1029/2000JD000037.

Quinn, P. K., D. J. Coffman, T. S. Bates, E. J. Welton, D. S. Covert, T. L. Miller, J. E. Johnson, S. Maria, L. Russell, R. Arimoto, C. M. Carrico, M. J. Rood, and J. Anderson (2004), Aerosol optical properties measured on board the *Ronald H. Brown* during ACE-Asia as a function of aerosol chemical composition and source region, *J. Geophys. Res., 109(D19),* doi:10.1029/2003JD004010.

Rivera Rivera, N. I., T. E. Gill, K. A. Gebhart, J. L. Hand, M. P. Bleiweiss, and R. M. Fitzgerald (2009), Wind modeling of Chihuahuan Desert dust outbreaks, *Atmos. Environ., 43,* 347-354.

Schichtel B. A., K. A. Gebhart, M. G. Barna and W. C. Malm (2006), Association of airmass transport patterns and particulate sulfur concentrations at Big Bend National Park, Texas, *Atmos. Environ., 40,* 992-1006.

Schwab, J. J., H. D. Felton, and K. L. Demerjian (2004), Aerosol chemical composition in New York state from integrated filter samples: Urban/rural and seasonal contrasts, *J. Geophys. Res., 109(D16),* doi:10.1029/2003JD004078.

Seinfeld, J. H., and S. N. Pandis (1998), *Atmospheric Chemistry and Physics: From Air Pollution to Climate Change,* John Wiley, New York.

Tanner, R. L., W. J. Parkhurst, M. L. Valente, and W. D. Phillips (2004), Regional composition of $PM_{2.5}$ aerosols measured at urban, rural, and "background" sites in the Tennessee valley, *Atmos. Environ., 38,* 3143-3153.

Turpin, B. J., P. Saxena, and E. Andrews (2000), Measuring and simulating particulate organics in the atmosphere: Problems and prospects, *Atmos. Environ., 34,* 2983-3013.

Turpin, B. J., and H.-J. Lim (2001), Species contributions to $PM_{2.5}$ mass concentrations: Revisiting common assumptions for estimating organic mass, *Aerosol Sci. Technol., 35,* 602-610.

VanCuren, R. A., and T. A. Cahill (2002), Asian aerosols in North America: Frequency and concentration of fine dust, *J. Geophys. Res., 107(D24),* 4804, doi:10.1029/2002JD002204.

VanCuren, R. A. (2003), Asian aerosols in North America: Extracting the chemical composition and mass concentration of the Asian continental aerosol plume from long-term aerosol records in the western United States, *J. Geophys. Res.,108(D20),* 4623, doi:10.1029/2003JD003459.

Van Vaeck, L., and K. Van Cauwenberghe (1978), Cascade impactor measurements of the size distribution of the major classes of organic pollutants in atmospheric particulate matter, *Atmos. Environ., 12,* 2239.

Vitousek, P. M., J. D. Aber, R. W. Howarth, G. E. Likens, P. A. Matson, D. W. Schindler, W. H. Schlesinger, and D. G. Tilman (1997), Human alteration of the global nitrogen cycle: Sources and consequences, *Ecolog. Applic. 7*(3), 737-750.

White, W. H., and P. T. Roberts (1977), On the nature and origins of visibility-reducing aerosols in the Los Angeles Air Basin, *Atmos. Environ., 11,* 803-812.

White, W. H. (2008), Chemical markers for sea salt in the IMPROVE aerosol data, *Atmos. Environ., 42,* 261-274.

Zhang, Q., M. R. Canagaratna, J. T. Jayne, D. R. Worsnop, and J.-L. Jimenez (2005), Time- and size-resolved chemical composition of submicron particles in Pittsburgh: Implications for aerosol sources and processes, *J. Geophys. Res., 110(D07),* doi:10.1029/2004JD004649.